The structure of low-lying excited states of spherical nuclei

V. Yu. Ponomarev
Joint Institute for Nuclear Research, Dubna

Fiz. Élem. Chastits At. Yadra **29**, 1354–1404 (November–December 1998)

The change of the structure of low-lying excited states of even–even spherical nuclei in going from closed-shell to transitional nuclei is studied using the quasiparticle–phonon model. The transition charge densities of these states and the distribution of electromagnetic transition strengths are investigated for excitation energies of up to 5 MeV. The properties of low-lying 1^- states and states forming pygmy resonances are analyzed. The anomalous behavior of the photoexcitation cross sections of isomers in odd nuclei is explained. The theoretical results are compared to the available experimental data. © *1998 American Institute of Physics.* [S1063-7796(98)00206-X]

INTRODUCTION

The development of modern technology has made it possible to design experimental setups and detectors with record-setting performance. In the last decade this has led to great progress in a traditional area of the physics of nuclear structure: nuclear spectroscopy. A striking example is the experiments using the new generation of germanium detectors, which have resulted in the discovery of more than fifty previously unknown levels in each isotope studied. The body of data obtained for various nuclear reactions allows the complete description of the nuclear spectroscopy for many nuclei up to excitation energies of several MeV. Comparison of the characteristics of closely spaced isotopes shows that the properties of a system change fundamentally when only two nucleons are added to the system. This cannot be attributed to a smooth change of global nuclear characteristics such as the mean field.

The wealth of new experimental data on the properties of low-lying nuclear states has stimulated theoretical studies. In the present review we systematize the results of the studies performed during the last decade using the quasiparticle–phonon model of the nucleus. Because the region of nuclear spectroscopy has been extended to energies at which not only two-phonon but also three- and four-phonon configurations are located, it is quite obvious that it is impossible to describe the full set of experimental data if the individual features of particular configurations in specific nuclei or the interaction between them are neglected. We therfore pay special attention to the interaction of simple (one-phonon) and complex (multi-phonon) components of the wave functions of low-lying states.

This review is divided into five sections. In the first we briefly describe the formalism of the quasiparticle–phonon model of the nucleus as applied to this problem. The second is devoted to study of the transition charge densities of low-lying states extracted from inelastic electron scattering. There we also study in detail the changes in the structure of low-lying states in going away from a closed shell. In the third section we consider the distribution of the isoscalar electromagnetic transition strength of transitions of various multipole orders for excitation energies of up to 5 MeV. The corresponding experimental data were obtained from inelastic proton and deuteron scattering. The reasons for the unsatisfactory description of these data for states of positive parity by the phenomenological interacting-boson model are discussed. The fourth section is devoted to the description of low-lying 1^- states. The fine structure of pygmy resonances is calculated. In addition, we study $E1$ transitions between low-lying states which are forbidden in the model of ideal bosons. Finally, in the fifth section we discuss some problems concerning the structure of low-lying states in odd nuclei. Special attention is paid to the theoretical interpretation of the isomer photoexcitation process.

1. THE FORMALISM OF THE QUASIPARTICLE–PHONON MODEL OF THE NUCLEUS

The Hamiltonian H of the quasiparticle–phonon model (QPM) of the nucleus[1–3] is chosen on the basis of physical considerations about the nucleons moving in a mean field and interacting with each other via the residual interaction. It can be written schematically as

$$H=H_{\text{m.f.}}+H_{\text{pair}}+H_{\text{r.i.}}. \tag{1}$$

The first term $H_{\text{m.f.}}$ corresponds to the mean field for neutrons (n) and protons (p). The second term H_{pair} is the interaction leading to pairing correlations of the superconductor type in monmagic nuclei. In the QPM this interaction is described as monopole pairing with constant matrix element $G_\tau^{(0)}$. The residual interaction $H_{\text{r.i.}}$ is chosen to be separable in the form of a multipole expansion.

The basic equations of the QPM are obtained by step-by-step diagonalization of the model Hamiltonian (1). In the first step the first two terms are diagonalized, assuming that the ground state of an even–even nucleus is the quasiparticle vacuum $|\,\rangle_q$. For this we make a canonical Bogolyubov transformation from the particle creation (annihilation) operators to the quasiparticle creation (annihilation) operators α_{jm}^+ (α_{jm}):

$$a_{jm}^+=u_j\alpha_{jm}^+ +(-1)^{j-m}v_j\alpha_{j-m}. \tag{2}$$

The result of this diagonalization is the well known BCS equations. By solving them we obtain the spectrum of one-quasiparticle excitations ε_j and the coefficients u_j and v_j of the Bogolyubov transformation.

We have defined the ground state of an even–even nucleus as the quasiparticle vacuum. In this case the simplest excited states of such a nucleus are two-quasiparticle states $\alpha^+_{jm}\alpha^+_{j'm'}|\,\rangle_q$ corresponding to a hole–particle type of transition. The two half-integer angular momenta of the quasiparticle fermionic operators are coupled to form an integer total angular momentum corresponding to Bose statistics, and so it is useful to project the bifermionic operators $[\alpha^+_j\alpha^+_{j'}]_{\lambda\mu}$ and $[\alpha_{j'}\alpha_j]_{\lambda-\mu}$ onto the space of quasibosonic operators, i.e., phonons. In making this "bosonic mapping," we introduce phonon operators of multipole order λ with projection μ as follows:

$$Q^+_{\lambda\mu i}=\frac{1}{2}\sum_{\tau}^{n,p}\sum_{jj'}\{\psi^{\lambda i}_{jj'}[\alpha^+_j\alpha^+_{j'}]_{\lambda\mu} -(-1)^{\lambda-\mu}\varphi^{\lambda i}_{jj'}[\alpha_{j'}\alpha_j]_{\lambda-\mu}\}. \quad (3)$$

The number of phonons of a given multipole order must coincide with the sum of neutron and proton two-quasiparticle states. The superscript i is introduced to distinguish between phonons of a given multipole order.

We obtain the spectrum of one-phonon excitations $\omega_{\lambda i}$ and coefficients $\psi^{\lambda i}_{jj'}$ and $\varphi^{\lambda i}_{jj'}$ of the transformation (3) by diagonalizing our model Hamiltonian in the space of one-phonon states $Q^+_{\lambda\mu i}|\,\rangle_{\rm ph}$. As a result, we find the well known equations of the random-phase approximation (RPA).

The introduction of phonon operators and the diagonalization of the model Hamiltonian on the basis of one-phonon states allows it to be rewritten as

$$H=\sum_{\lambda\mu i}\omega_{\lambda i}Q^+_{\lambda\mu i}Q_{\lambda\mu i}+H_{\rm int}, \quad (4)$$

$$H_{\rm int}=-\frac{1}{2}\sum_{\lambda\mu i}\left\{[(-1)^{\lambda-\mu}Q^+_{\lambda\mu i}+Q_{\lambda-\mu i}] \times\sum_{jj'\tau}\frac{f^{\lambda}_{jj'}v^{(-)}_{jj'}}{\sqrt{2\mathscr{Y}^{\lambda i}_{\tau}}}B_{\tau}(jj';\lambda-\mu)+{\rm H.c.}\right\}, \quad (5)$$

$$B_{\tau}(jj';\lambda\mu)=\sum_{mm'}(-1)^{j'+m'}C^{\lambda\mu}_{jmj'm'}\alpha^+_{jm}\alpha_{j'-m'}, \quad (6)$$

where $1/\sqrt{2\mathscr{Y}^{\lambda i}_{\tau}}$ is a normalization factor. The term $H_{\rm int}$ in (4) ensures the interaction of configurations differing from each other in the number of phonons.

Now let us write down the wave function of an excited state of an even–even nucleus of multipole order J^{π} as a superposition of configurations containing different numbers of phonons:

$$\Psi^{\nu}(JM)=\left\{\sum_{\alpha_1}S^{\nu}_{\alpha_1}(J)Q^+_{\alpha_1}+\sum_{\alpha_2\beta_2}\frac{D^{\nu}_{\alpha_2\beta_2}(J)}{\sqrt{1+\delta_{\alpha_2,\beta_2}}} \times[Q^+_{\alpha_2}Q^+_{\beta_2}]_{JM}+\sum_{\alpha_3\beta_3\gamma_3}\frac{T^{\nu}_{\alpha_3\beta_3\gamma_3}(J)}{\sqrt{1+\delta_{\alpha_3,\beta_3,\gamma_3}}} \times[Q^+_{\alpha_3}Q^+_{\beta_3}Q^+_{\gamma_3}]_{JM}+\cdots\right\}|\,\rangle_{\rm ph},$$

$$\delta_{\alpha_3,\beta_3,\gamma_3}=\delta_{\alpha_3,\beta_3}+\delta_{\alpha_3,\gamma_3}+\delta_{\beta_3,\gamma_3}+2\delta_{\alpha_3,\beta_3}\delta_{\alpha_3,\gamma_3}. \quad (7)$$

The Greek letters α, β, and γ denote combinations of indices $\{\lambda i\}$, and ν numbers the different states described by the wave function (7) with given angular momentum and parity. In (7) it is understood that any combination $\{\alpha,\beta,\gamma\}$ is encountered only once. Beginning with the two-phonon part, the wave function (7) contains phonons of arbitrary multipole order; only the fact that they add to form total angular momentum J is important.

Let us restrict ourselves to three-phonon terms in the excited-state wave function. Then, using the minimization procedure

$$\delta\{\langle\Psi^{\nu}(JM)|H|\Psi^{\nu}(JM)\rangle-E^J_x\langle\Psi^{\nu}(JM)|\Psi^{\nu}(JM)\rangle\}=0, \quad (8)$$

we obtain a system of linear equations for the eigenvalues in terms of the coefficients $S^{\nu}_{\alpha_1}(J)$, $D^{\nu}_{\alpha_2\beta_2}(J)$, and $T^{\nu}_{\alpha_3\beta_3\gamma_3}(J)$:

$$(\omega_{\alpha_1}-E^J_x)S^{\nu}_{\alpha_1}(J)+\sum_{\alpha_2,\beta_2}D^{\nu}_{\alpha_2\beta_2}(J)\tilde{U}^{\alpha_1}_{\alpha_2\beta_2}=0,$$

$$\sum_{\alpha_1}S^{\nu}_{\alpha_1}(J)\tilde{U}^{\alpha_1}_{\alpha_2\beta_2}+(\omega_{\alpha_2}+\omega_{\beta_2}+\Delta\omega^J_{\alpha_2\beta_2}-E^J_x)D^{\nu}_{\alpha_2\beta_2}(J) +\sum_{\alpha_3\beta_3\gamma_3}T^{\nu}_{\alpha_3\beta_3\gamma_3}(J)\tilde{U}^{\alpha_2\beta_2}_{\alpha_3\beta_3\gamma_3}=0,$$

$$\sum_{\alpha_2\beta_2}D^{\nu}_{\alpha_2\beta_2}(J)\tilde{U}^{\alpha_2\beta_2}_{\alpha_3\beta_3\gamma_3}+(\omega_{\alpha_3}+\omega_{\beta_3}+\omega_{\gamma_3}+\Delta\omega^J_{\alpha_3\beta_3\gamma_3} -E^J_x)T^{\nu}_{\alpha_3\beta_3\gamma_3}(J)=0, \quad (9)$$

where

$$\tilde{U}^{\alpha_1}_{\alpha_2\beta_2}=\frac{1}{2}\sqrt{1+\delta_{\alpha_2,\beta_2}}\langle Q_{\alpha_1}|H_{\rm int}|[Q^+_{\alpha_2}Q^+_{\beta_2}]_{JM}\rangle,$$

$$\tilde{U}^{\alpha_2\beta_2}_{\alpha_3\beta_3\gamma_3}=\frac{1}{2}\sqrt{1+\delta_{\alpha_2,\beta_2}}\sqrt{1+\delta_{\alpha_3,\beta_3,\gamma_3}} \times\langle[Q_{\alpha_2}Q_{\beta_2}]_{JM}|H_{\rm int}|[Q^+_{\alpha_3}Q^+_{\beta_3}Q^+_{\gamma_3}]_{JM}\rangle \quad (10)$$

are the matrix elements of the interaction of phonon configurations with number of phonons differing by unity. In obtaining (9) we neglected the matrix elements of the interaction of one- and three-phonon configurations, which are of next order in smallness compared to the matrix elements of one-phonon exchange. The energy shifts of the two- and three-phonon configurations $\Delta\omega^J_{\alpha_2\beta_2}$ and $\Delta\omega^J_{\alpha_3\beta_3\gamma_3}$ are due to the fermionic structure of the phonon operators. Technically, this

implies that in calculating the eigenenergies of these configurations we have used the exact, rather than bosonic, commutation relations:

$$[Q_{\lambda\mu i}, Q^{+}_{\lambda'\mu' i'}]_{-} = \delta_{\lambda,\lambda'}\delta_{\mu,\mu'}\delta_{i,i'} \times \frac{1}{2}\sum_{jj'}[\psi^{\lambda i}_{jj'}\psi^{\lambda i'}_{jj'} - \varphi^{\lambda i}_{jj'}\varphi^{\lambda i'}_{jj'}] - \sum_{jj'j_2}\sum_{mm'm_2}\alpha^{+}_{jm}\alpha_{j'm'} \times \{\psi^{\lambda i}_{j'j_2}\psi^{\lambda' i'}_{jj_2}C^{\lambda\mu}_{j'm'j_2m_2}C^{\lambda'\mu'}_{jmj_2m_2} - (-)^{\lambda+\lambda'+\mu+\mu'} \times \varphi^{\lambda i}_{jj_2}\varphi^{\lambda' i'}_{j'j_2}C^{\lambda-\mu}_{jmj_2m_2}C^{\lambda'-\mu'}_{j'm'j_2m_2}\}. \quad (11)$$

The same commutation relations (11) are used to obtain the matrix elements $\tilde{U}^{\alpha_1}_{\alpha_2\beta_2}$ and $\tilde{U}^{\alpha_2\beta_2}_{\alpha_3\beta_3\gamma_3}$. Both the matrix elements $\tilde{U}$ and the energy shifts of multiphonon configurations $\Delta\omega^J$ are complicated functions of the amplitudes ψ and φ of the phonons entering into them. Since they are cumbersome we do not give them here, and refer the reader to, for example, Ref. 3 for their explicit expressions.

The rank of the system (9) is determined by the number of one-, two-, and three-phonon configurations included in the wave function (7). As a rule, when describing the properties of low-lying states it is possible, guided by physical arguments, to make a reasonable cutoff of the multiphonon configuration basis and restrict ourselves to 1000–2000 linear equations of the system (9). This system can then be solved numerically for the eigenvalues by diagonalizing the matrix, giving the set of eigenvalues E^{ν}_{x} of states described by the wave function (7), and also the eigenvectors or the coefficients $S^{\nu}_{\alpha_1}(J)$, $D^{\nu}_{\alpha_2\beta_2}(J)$, and $T^{\nu}_{\alpha_3\beta_3\gamma_3}(J)$.

Equations (9) represent the basic equations for calculating the excited-state spectra of even–even spherical nuclei, given below. The expressions for the various physical characteristics corresponding to physical excitations of these states in experiments (such as the reduced electromagnetic excitation probabilities or the reaction cross sections) will be given below when needed.

To perform actual calculations we need to define the parameters of the model Hamiltonian. In the QPM the mean field for neutrons and protons is described by the phenomenological Woods–Saxon potential. Practically all the calculations given in this review were performed using the parameters of this potential for various mass ranges taken from Ref. 4. In some cases, for example, in the calculations for ^{208}Pb, the energies of single-particle levels near the Fermi surface were varied slightly to obtain a more accurate description of the spectra of low-lying states in the neighboring odd nuclei. In the calculations we used all the bound and quasi-bound states with small width of the Woods–Saxon potential. The monopole pairing parameters for neutrons and protons $G^{(0)}_{\tau}$ were determined from the description of the pairing energies. Their values are also given in Ref. 4. The parameters $\varkappa^{(\lambda)}_{0(1)}$ describing the strength of the residual isoscalar (isovector) interaction were selected so as to correctly describe the collective nature, i.e., the value of B(Eλ) for the lowest states of various multipole orders with $\lambda \geq 2$ in even–even nuclei. Here we took $\varkappa^{(\lambda)}_{1} = -1.2\varkappa^{(\lambda)}_{0}$. For $\lambda = 1$ the parameters $\varkappa^{(1)}_{1}$ and $\varkappa^{(1)}_{0}$ were defined so as to describe the location of the giant dipole resonance and exclude the ghost state.

The main difficulty with the numerical calculations using the wave functions (7) is the high density of multiphonon configurations. We therefore were guided by physical considerations and included only those configurations which play a significant role. The multiphonon components in the wave functions (7) will be selected using the following considerations. First, we want to exclude configurations located far from the energy range studied. Second, we want to exclude multiphonon configurations which are formed only from noncollective phonons. For this we need to introduce a numerical criterion for phonons to be collective. We shall consider a phonon to be noncollective if one of the two-quasiparticle components entering into its structure contributes more than 50–60% to its normalization. Multiphonon configurations formed only from noncollective phonons have matrix element U of the interaction with other configurations which is many times smaller than that for the analogous configurations containing collective phonons. Therefore, noncollective multiphonon configurations practically do not mix with one-phonon configurations and do not affect their properties.

2. THE STRUCTURE AND TRANSITION DENSITIES IN EVEN–EVEN SPHERICAL NUCLEI

The inelastic scattering of electrons on nuclei is one of the most suitable processes for studying nuclear structure, because the interaction of the electron beam with the target is purely electromagnetic in nature. Knowledge of the reaction mechanism makes it possible to extract information about nuclear excited states from the scattering cross sections by a model-independent analysis. In the last decade, the use of high-resolution spectrometers in the (e,e') reaction has allowed the detailed study of the structure of excited states of heavy nuclei up to 3–4 MeV as a function of the density of states in each specific nucleus. The experimental data are analyzed as follows. Measurements are made at several values of the momentum transfer (as a rule, this is regulated by changing the beam energy and the scattering angle). The location of the first maximum of the cross section is used to determine the multipole order of each excited state resolved experimentally. For each state the dependence of the cross section on the momentum transfer is fitted by distorted-wave calculations using the transition density of the excited stated, specified parametrically as

$$\rho_{\lambda}(r) = \begin{cases} \sum_{\mu=1}^{\mu_{\max}} A_{\mu} q_{\mu}^{\lambda-1} j_{\lambda}(q_{\mu}^{\lambda-1} r) & (r < R_c) \\ 0 & (r \geq R_c), \end{cases} \quad (12)$$

where A_{μ} are fitted parameters and $j_{\lambda}(qr)$ are Bessel functions of order λ. The quantities $q_{\mu}^{\lambda-1}$ are determined from the relation $j_{\lambda-1}(q_{\mu}^{\lambda-1}R_c) = 0$. A sufficiently large value is

chosen for R_c, several times larger than the nuclear radius, and usually $\mu_{\max}\approx 15$ is used. The parameters A_μ for the chain of neodymium isotopes are given in Ref. 5.

The transition charge densities (12) extracted from experiment in this model-independent manner can be directly compared to the corresponding characteristics of the excited states predicted by various nuclear models. The transition density of an excited nuclear state is a characteristic which indicates how the shape of the nucleus changes in going from the ground state to the excited state. It therefore contains detailed information about the changes in the radial structure of the nucleus, whereas integrated characteristics like the reduced transition probabilities B(Eλ) and B(Mλ), related to the transition densities as

$$B(E\lambda)=\frac{2J_f+1}{2J_i+1}\left[\int_0^\infty \rho_\lambda(r)r^{\lambda+2}dr\right]^2, \tag{13}$$

are mainly sensitive only to the behavior of the transition densities near the nuclear surface. The degree to which a given state is collective can be judged from the shape of the transition density. For low-lying states, collective excitations correspond to transition densities with a well defined maximum near the nuclear surface, while the transition densities of two-quasiparticle excitations have a maximum inside the nucleus. Naturally, comparison of the calculated transition densities with the experimental data provides a very sensitive test of the available nuclear models.

As noted above, the transition charge density is defined as the overlap of the nuclear wave functions in the ground and excited states:

$$\rho(\mathbf{r})=\langle\Psi_f|\sum_k \delta(\mathbf{r}-\mathbf{r}_k)|\Psi_i\rangle, \tag{14}$$

where the integration runs over all the internal coordinates, including r_k. Since nuclear excited states possess definite angular momentum and parity, it is useful to make a multipole expansion of (14) and to introduce the transition density of multipole order λ:

$$\rho(\mathbf{r})=e\sum_{\lambda\mu}(-i)^\lambda C^{J_fM_f}_{J_iM_i,\lambda\mu}Y^\dagger_{\lambda\mu}(\mathbf{r})\rho_\lambda(r),$$

$$\rho_\lambda(r)=\langle\Psi_f||\sum_k r_k^{-2}\delta(r-r_k)(-i)^\lambda Y^\dagger_\lambda(\mathbf{r}_k)||\Psi_i\rangle. \tag{15}$$

Multiplying (14) by $i^\lambda Y_{\lambda\mu}(\mathbf{r})$, substituting the phonon vacuum for the ground-state wave function and (7) for the excited-state wave function, and integrating over angles, we obtain the model expression for the transition density corresponding to an excited state of an even–even nucleus described by the wave function (7):

$$\rho^\nu_\lambda(r)=\sum_i S^\nu_i(\lambda)\rho^i_\lambda(r)+\sum_{\lambda_1 i_1\lambda_2 i_2}\frac{D^\nu_{\lambda_1 i_1\lambda_2 i_2}(\lambda)}{\sqrt{1+\delta_{\lambda_1 i_1,\lambda_2 i_2}}}\times\rho^{\lambda_1 i_1\lambda_2 i_2}_\lambda(r)+\sum_{\alpha_3\beta_3\gamma_3}\frac{T^\nu_{\alpha_3\beta_3\gamma_3}(\lambda)}{\sqrt{1+\delta_{\alpha_3,\beta_3,\gamma_3}}}\rho^{\alpha_3\beta_3\gamma_3}_\lambda(r). \tag{16}$$

The transition density of the ith one-phonon component of multipole order λ has the form

$$\rho^i_\lambda(r)=\sum_{jj'}\rho^\lambda_{jj'}(r)\frac{u^{(+)}_{jj'}}{2}(\psi^{\lambda i}_{jj'}+\varphi^{\lambda i}_{jj'}). \tag{17}$$

For the transition density of the two-phonon component $[\lambda_1 i_1\otimes\lambda_2 i_2]_\lambda$ we find

$$\rho^{\lambda_1 i_1\lambda_2 i_2}_\lambda(r)=-\sum_{jj'j''}\sum_{\lambda_1 i_1\lambda_2 i_2}\sqrt{(2\lambda_1+1)(2\lambda_2+1)}\times\begin{Bmatrix} j & j' & j''\\ \lambda_1 & \lambda_2 & \lambda\end{Bmatrix}v^{(-)}_{jj'}(\psi^{\lambda_1 i_1}_{j'j''}\varphi^{\lambda_2 i_2}_{j''j}+\varphi^{\lambda_1 i_1}_{j'j''}\psi^{\lambda_2 i_2}_{j''j})\rho^\lambda_{jj'}(r). \tag{18}$$

Equations (17) and (18) are functions of the phonon amplitudes ψ and φ, and also of the two-quasiparticle transition densities

$$\rho^\lambda_{jj'}(r)=(-1)^{j-1/2}i^{l'-l-\lambda}\frac{\hat j\hat j'}{\hat\lambda 4\sqrt{\pi}}(1+(-1)^{l+l'+\lambda})\times C^{\lambda 0}_{j(1/2)j'-1/2}R^\dagger_j(r)R_{j'}(r), \tag{19}$$

where $R^\dagger_j(r)$ is the radial part of the single-particle wave function. Here we have used the notation $\hat\lambda=\sqrt{2\lambda+1}$. We shall not give the expression for the transition density of the three-phonon component, since it is of next order in smallness even compared to the transition density of the two-phonon components. Accordingly, we have assumed that $\rho^{\alpha_3\beta_3\gamma_3}_\lambda(r)=0$ directly in the numerical calculations.

For the detailed study of how the properties of low-lying states change in going from closed-shell nuclei to transitional nuclei, the best objects are nuclei for which fairly long isotope chains exist in nature. The presence of such chains allows comparison of the theoretical predictions with the experimental data for all the isotopes studied.

One such chain is that of neodymium (Nd) isotopes. Experimental data on electron inelastic scattering with the excitation of low-lying states for this chain have been obtained at the electron accelerator at NIKHEF (Amsterdam).[6–9] The beam energy varied from 112 to 450 MeV, covering the range of momentum transfers from 0.5 to 2.8 F^{-1}. The enriched isotopes ^{142}Nd, ^{144}Nd, and ^{146}Nd were used as targets. Excited states were resolved experimentally up to 3.5 MeV with momentum and parity varying from 0^+ to 9^-. The structure of the excited states and the transition densities were calculated theoretically using the formalism described in Sec. 1. In the numerical calculations we used the single-particle spectrum of the Woods–Saxon potential. The parameters of this potential for the neutron scheme were taken from Ref. 4 and those for the proton scheme were taken from Ref. 10, selected using the experimental data on electron elastic scattering on Nd nuclei. The phonon basis was chosen as follows. We included both collective and noncollective one-phonon components of the wave function (7) up to

TABLE I. Energies and reduced excitation probabilities B(Eλ) of states of various multipole order in ^{142}Nd. The calculations were performed using the one-phonon approximation—the RPA, where i is the phonon order, and using the wave function (7)—the QPM, where ν is the order of the excited state of a given multipole order.

	Theory						Experiment	
	RPA			QPM				
λ^π	i	E_x, MeV	B(Eλ), $e^2F^{2\lambda+2}$	ν	E_x, MeV	B(Eλ), $e^2F^{2\lambda+2}$	E_x, MeV	B(Eλ), $e^2F^{2\lambda+2}$
2^+	1	1.90	0.382×10^4	1	1.63	0.406×10^4	1.58	0.281×10^4
	2	2.48	0.124×10^3	2	2.42	0.248×10^3	2.39	0.309×10^3
	3	2.60	0.269×10^3	3	2.53	0.173×10^3		
	4	3.30	0.133×10^4	4	3.05	0.705×10^3	2.85	0.498×10^3
	5	3.83	0.330×10^1	5	3.32	0.990×10^2	3.05	
	6	3.94	0.500×10^0	6	3.92	0.398×10^2		
3^-	1	2.50	0.200×10^6	1	2.05	0.185×10^6	2.08	0.262×10^6
	2	3.37	0.110×10^4	2	3.28	0.236×10^4		
				3	4.01	0.132×10^5	3.58	0.100×10^5
	3	4.83	0.537×10^5	4	4.71	0.404×10^5		
4^+	1	2.28	0.173×10^7	1	2.16	0.195×10^7	2.10	0.450×10^7
	2	2.48	0.650×10^6	2	2.43	0.776×10^6	2.44	0.210×10^6
	3	2.67	0.410×10^6	3	2.63	0.337×10^6	2.58	0.700×10^5
	4	3.63	0.347×10^7	4	3.16	0.148×10^7	3.08	0.620×10^6
	5	3.93	0.360×10^6	5	3.46	0.145×10^7	3.32	0.114×10^7
	6	4.03	0.800×10^5	6	3.70	0.222×10^6		
	7	4.08	0.200×10^5	7	3.99	0.464×10^5		
5^-	1	3.00	0.174×10^9	1	2.67	0.158×10^9	2.74	0.121×10^9
	2	3.34	0.100×10^8	2	3.25	0.190×10^9		
	3	4.58	0.750×10^8	3	3.84	0.950×10^6		
6^+	1	2.30	0.863×10^{10}	1	2.21	0.861×10^{10}	2.21	0.940×10^{10}
	2	2.69	0.150×10^9	2	2.65	0.850×10^9	2.89	0.800×10^8
	3	3.99	0.235×10^{10}	3	3.73	0.226×10^{10}	3.41	0.200×10^{10}
7^-	1	3.16	0.148×10^{12}	1	2.92	0.135×10^{12}	3.25	0.250×10^{12}
	2	3.34	0.650×10^{11}	2	3.25	0.750×10^{11}		

4.5 MeV, two-phonon components up to 6.5 MeV, and three-phonon components constructed from 2_1^+, 3_1^-, and 4_1^+ phonons.

The results[7] for the spectrum of excited states and reduced transition probabilities B(Eλ) in the semimagic isotope ^{142}Nd calculated using the wave function (7) are given in Table I. For comparison, in the same table we also give the results calculated in the one-phonon approximation and the experimental data. The transition charge densities predicted by our calculations and obtained by processing the cross sections for the (e,e') reaction are shown in Fig. 1.

It is not possible to reconstruct the transition density by a model-independent analysis for all the states extracted experimentally. As a rule, problems arise owing to admixtures of states of different multipole order, which, in spite of the high spectrometer resolution, cannot be separated. In such cases the state seen experimentally is given only in the table; very often this state, and also its spin and parity, are known from other experiments, and from the amplitude of its form factor in the (e,e') reaction it is possible to assign a value of B(Eλ) corresponding to its excitation in this reaction.

The quasiparticle–phonon model predicts that ^{142}Nd has six quadrupole 2^+ states with excitation energy below 4 MeV. Their energies and reduced transition probabilities B(E2) are given in Table I. Since ^{142}Nd has a closed neutron shell, there is no monopole pairing in the neutron system. Therefore, the lowest particle–hole 2^+ configuration has energy higher than 5 MeV. The proton components thus dominate in all the one-phonon 2^+ states in Table I. The 2_1^+ state is the most strongly collectivized. The 2_2^+ and 2_3^+ states are almost pure two-quasiparticle states and are characterized by very small values of B(E2). However, the 2_4^+ state is again collective, and its value of B(E2) is only a third of that of the 2_1^+ state. This difference in the collective nature of 2^+ phonons is also reflected in their transition charge densities. The transition densities of the 2_1^+ and 2_4^+ states have maxima near the nuclear surface, while the transition densities of the 2_2^+ and 2_3^+ states are characterized by expressed peaks inside the nucleus. The reason for the distribution of collectivization among the low-lying 2^+ is buried in the shell structure. The two proton subshells near the Fermi surface, $1g_{7/2}$ and $2d_{5/2}$, are located close to each other, whereas the other subshells, namely, $1h_{11/2}$, $2d_{3/2}$, and $3s_{1/2}$, have a single-particle energy roughly 2 MeV larger. This means that the quasiparticle energies of these levels are about 1 MeV higher than for the $1g_{7/2}$ and $2d_{5/2}$ levels. This effect is also observed in states of odd nuclei. The 2_4^+ state contains

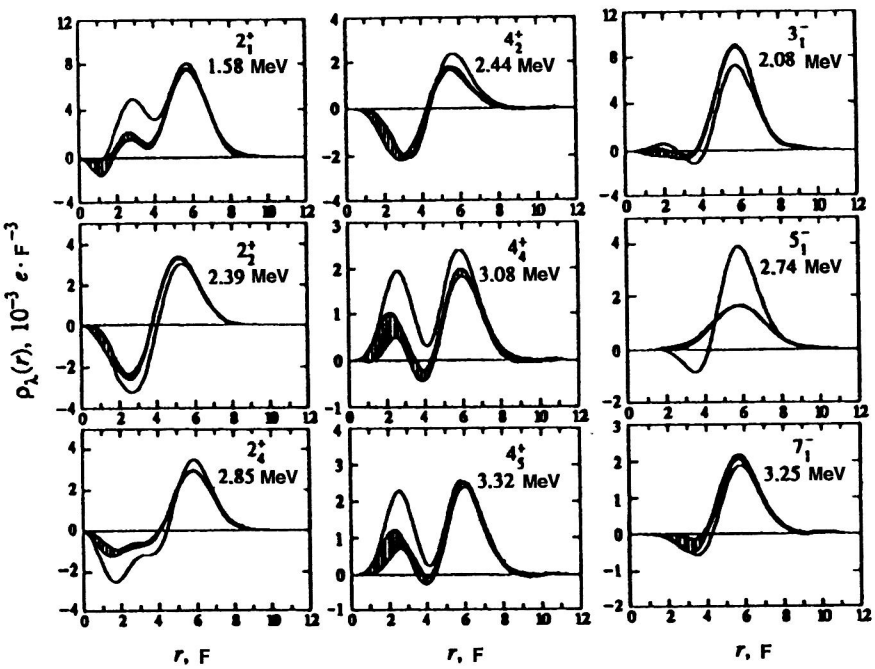

FIG. 1. Transition charge densities of several low-lying excited states in ^{142}Nd. The curves with the experimental errors correspond to the densities extracted by a model-independent analysis from the cross sections for electron inelastic scattering, and the solid lines are the predictions of our calculations. The indicated excitation energies correspond to the experimental values.

mainly the strength of two-quasiparticle configurations located at higher energy, and owing to the energy gap is much more collectivized than the 2_2^+ and 2_3^+ states. The one-phonon 2_5^+ and 2_6^+ states are again noncollective.

After the mixing of the one-, two-, and three-phonon configurations in the wave function (7), we again obtain six 2^+ states with energy below 4 MeV (see Table I). The matrix elements of the interaction between the one- and two-phonon configurations are small in ^{142}Nd, and no significant admixtures of three-phonon configurations are observed up to 3 MeV. This is the usual situation in semimagic nuclei.[11] The lowest two-phonon configuration $[2_1^+ \otimes 2_1^+]_{2^+}$ has energy 3.8 MeV, and the other two-phonon configurations are located above 4 MeV. One-phonon components (collective and noncollective) therefore dominate in the wave functions of 2^+ states below 3 MeV. Actually, the admixture of two-phonon components does not exceed a few percent for the four lowest 2^+ states. Since the absolute values of the transition densities of the two-phonon components is significantly smaller than those of the one-phonon components, the contribution of the admixture of two-phonon transition densities is practically insignificant. The mixing of the various one-phonon components in the wave function (7) and the renormalization of their contribution due to the two-phonon part of the wave function are more important. The transition densities of the lowest 2^+ states seen experimentally are compared to the predictions of our calculations in Fig. 1. In all probability, the state corresponding to the 2_3^+ state in the calculation was not seen owing to its small excitation probability.

Since the shapes of the transition charge densities of the various excited states differ significantly from each other, we can consider directly comparing the states observed experimentally and predicted theoretically. We can therefore state that our calculations correctly reproduce the systematics of excited 2^+ states. The transition densities of the one-phonon 2_1^+ and 2_4^+ components dominate in the transition densities of the corresponding states. The other components give a contribution of less than 1%, and add up to about 10%. The situation observed for the 2_2^+ and 2_3^+ states is different. Here the interaction with the two-phonon components leads to mixing of the one-phonon 2_2^+ and 2_3^+ components at a level of 10%. As a result, the value of B(E2) for the 2_2^+ state is increased, while that for the 2_3^+ state is decreased owing to destructive interference. This may be the reason why the 2_3^+ state was not observed experimentally. If the transition density of the 2_3^+ state is used to calculate the form factor, the cross section for the (e,e') reaction lies, within the experimental error, in the radiative tail of the strong peaks located at lower energies. A state with energy 2550 MeV has actually been discovered,[12] and its spin and parity are conjectured to be 2^+.

On the whole, the shapes of all three transition densities of 2^+ states found in inelastic electron scattering are in good agreement with the predictions of our calculations. The prediction and discovery of the collective 2_4^+ state is the most interesting. As noted above, this is a consequence of the energy gap in the single-particle spectrum $(1g_{7/2}, 2d_{5/2} \Leftrightarrow 1h_{11/2}, 2d_{3/2}, 3s_{1/2})$. A characteristic feature of our calculations is the overestimate of the amplitudes of the inner peaks of the transition densities. Inner peaks which are too strong are also present in the transition densities of the one-phonon components. The reason for this is that the contribution of the two-quasiparticle configuration $\pi(2d_{5/2}, 2d_{5/2})$ to the phonon structure is too large. This effect is seen even more clearly in the transition densities of 4^+ states. It has recently been shown that the inclusion of ground-state correlations beyond the RPA tends to decrease the contribution of the main two-quasiparticle configurations to the structure of the lowest collective phonons and thus

significantly improves the description of the inner part of the transition density of collective states.[13]

Let us now consider the 3^- excited states in ^{142}Nd. Only two one-phonon 3^- configurations have energy below 4 MeV. The energies and values of $B(E3)$ of these states are given in Table I. As in the case of quadrupole states, the main contribution to their structure comes from proton two-quasiparticle configurations. The first 3^- one-phonon state is strongly collectivized, in contrast to the second, which is practically a pure two-quasiparticle state. After including the interaction of one-phonon configurations with multiphonon ones, we obtain the spectrum of 3^- excitations, which is also given in Table I.

The 3^-_1 state is strongly collectivized; the one-phonon 3^-_1 configuration gives a contribution of roughly 84%, while the contribution of two-phonon configurations is about 10%. The 3^-_2 state remains practically a two-quasiparticle state. The third 3^- state is again a collective state, but the main contribution to its structure comes from the two-phonon configuration $[2^+_1 \otimes 3^-_1]_{3^-}$. As already noted, the transition densities of the two-phonon configurations are significantly smaller than those of the one-phonon ones, and so the transition density of the 3^-_3 state is considerably weaker than that of the 3^-_1 state.

Two 3^- states of energy 2.083 and 3.580 MeV were discovered in the $(e,e')^{142}$Nd experiment. However, owing to the absence of diffraction minima in the form factor of the second state, which most likely indicates that there is some admixture of states of a different multipole order, it was not possible to extract the transition density of this state. Therefore, theory and experiment for this state were compared at the level of the form factors, and good agreement was obtained. The problems with extracting the transition density for the lowest 3^- state were associated with the fact that the lowest 4^+ state in ^{142}Nd has excitation energy 2.098 MeV. The experimental resolution was not good enough to separate the 3^-_1 and 4^+_1 levels, which are separated by 15 keV. The experimental transition density of the 3^-_1 state, shown in Fig. 1, was obtained only after subtracting from the total form factor of the 3^-_1 and 4^+_1 levels the form factor of the 4^+_1 level calculated with the transition density in the form of the derivative of the mean field.

Our calculations predict five one-phonon 4^+ states in ^{142}Nd with energy below 4 MeV. Their energies and values of B(E4) are given in Table I. All these states, like the states of other multipole orders, consist practically of only proton two-quasiparticle configurations. The one-phonon 4^+_1 state is less strongly collective than the 2^+_1 and 3^-_1 phonons, and the main two-quasiparticle configuration $\pi(2d_{5/2}, 2d_{5/2})$ contributes roughly 90% of its structure. This is confirmed by the results of a proton inelastic scattering experiment[14] in which the atypical angular distribution of the 4^+_1 state of energy 2.098 MeV was explained by the presence of a large contribution to its structure from the two-quasiparticle component. The 4^+_2 and 4^+_3 states are nearly pure two-quasiparticle states. The next one-phonon 4^+_4 state, like the 2^+_4 state, manifests the properties of a strongly collectivized phonon, with a large number of different two-quasiparticle configurations contributing coherently to its structure, which causes the value of B(E4) for this state to be larger than the corresponding value for the lowest 4^+ phonon. Although many different two-quasiparticle configurations contribute to the structure of the 4^+_5 phonon, some of them interfere destructively, and so the value of B(E4) corresponding to this phonon is considerably smaller.

The interaction with complex configurations has practically no effect on the properties of the lowest three 4^+ states. Both the values of B(E4) given in Table I and the transition densities of these states are practically unchanged. However, the strength of the fourth 4^+ phonon is distributed between two states of energy 3.16 and 3.46 MeV. This occurs mainly owing to the interaction with the two-phonon configuration $[2^+_1 \otimes 2^+_1]_{4^+}$, which is close in energy to the 4^+_4 phonon. These two states have a similar structure: roughly 40% is from the 4^+_4 one-phonon configuration, 40% is from the above-mentioned two-phonon configuration, and 8% is from three-phonon configurations. As a result, the two states 4^+_4 and 4^+_5 have similar values of B(E4) and similar shapes of the transition charge density (see Table I and Fig. 1).

As mentioned above, since the 3^-_1 and 4^+_1 levels in ^{142}Nd are close, the transition density corresponding to the 4^+_1 level is not known experimentally. The transition density of the 4^+_2 level has the behavior characteristic of a noncollective excitation, and agrees well with the theoretical prediction. The most remarkable feature of the 4^+ excited states is the presence of two closely spaced levels, 4^+_4 and 4^+_5, whose transition densities are very similar. This completely corresponds to the theoretical predictions and is the result of the interaction between one-phonon and multiphonon configurations.

In going from semimagic nuclei to nuclei with nonclosed neutron and proton subshells, the collective nature of the lowest states is enhanced. This is especially true of the 2^+_1 state, whose excitation energy is also considerably lowered. The enhancement of the collective nature tends to increase the matrix element of the interaction of one-phonon configurations with more complex ones. The decrease of the excitation energy of the lowest one-phonon 2^+ configuration leads to a decrease of the energy separation of the lowest one- and two-phonon configurations, and so on. These two effects operate in the same direction and lead to stronger mixing of phonon configurations of various complexity in nuclei with a non-closed shell. Let us discuss in more detail the location, structure, and transition charge densities of low-lying states of nonmagic nuclei for the example of the ^{144}Nd isotope.[8]

For ^{144}Nd our calculations predict the presence of eight one-phonon 2^+ configurations with excitation energy below 4 MeV. Of course, the first of these is the most strongly collectivized. It has excitation energy 1.48 MeV and B(E2) $=4.4\times10^3\ e^2\mathrm{F}^4$. The fifth one-phonon configuration with $E_x=3.3$ MeV and B(E2)$=1.1\times10^3\ e^2\mathrm{F}^4$ is also collective, and the other one-phonon 2^+ configurations are practically purely two-quasiparticle ones. The collective nature of the lowest four one-phonon configurations is clearly seen from the shape of their transition densities. The transition density of the one-phonon 2^+_1 configuration has a prominent peak at the nuclear surface, and the others have a shape characteristic

TABLE II. Excitation energies, reduced transition probabilities B(E2), and principal components of the wave functions of low-lying 2^+ states in ^{144}Nd.

	Experiment		Theory				
λ^π_ν	E_x, MeV	B(E2), e^2F^4	E_x, MeV	B(E2), e^2F^4	Q^+ Comp.	Q^+Q^+ Comp.	$Q^+Q^+Q^+$ Comp.
2^+_1	0.696	4.60×10^3	0.708	3.8×10^3	$2^+_1-78\%$	$[2^+_1\otimes4^+_1]_{2^+}-6\%$ $[3^-_1\otimes3^-_1]_{2^+}-4\%$ $[3^-_1\otimes5^-_1]_{2^+}-4\%$	2%
2^+_2			1.575	7.9×10^1	$2^+_2-10\%$ $2^+_4-4\%$	$[2^+_1\otimes2^+_1]_{2^+}-63\%$	19%
2^+_3	2.073	6.31×10^2	2.105	1.5×10^2	$2^+_2-70\%$	$[2^+_1\otimes2^+_1]_{2^+}-7\%$ $[2^+_1\otimes4^+_1]_{2^+}-10\%$ $[3^-_1\otimes5^-_1]_{2^+}-2\%$	5%
2^+_4	2.368	2.38×10^2	2.440	2.0×10^2	$2^+_3-87\%$ $2^+_4-2\%$	$[2^+_1\otimes4^+_1]_{2^+}-4\%$	2%
2^+_5	2.527	3.47×10^2	2.528	2.2×10^2	$2^+_1-2\%$ $2^+_3-6\%$ $2^+_4-77\%$ $2^+_5-3\%$	$[2^+_1\otimes4^+_1]_{2^+}-4\%$ $[2^+_1\otimes4^+_4]_{2^+}-3\%$	2%
2^+_6			2.864	1.0×10^2	$2^+_1-5\%$ $2^+_2-10\%$ $2^+_3-3\%$ $2^+_4-11\%$ $2^+_5-13\%$	$[2^+_1\otimes2^+_1]_{2^+}-2\%$ $[2^+_1\otimes4^+_1]_{2^+}-40\%$	15%
2^+_7			3.013	1.1×10^2	$2^+_1-2\%$ $2^+_2-3\%$ $2^+_5-44\%$	$[2^+_1\otimes4^+_1]_{2^+}-8\%$ $[2^+_1\otimes4^+_5]_{2^+}-3\%$ $[3^-_1\otimes3^-_1]_{2^+}-21\%$	14%
2^+_8			3.354	3.6×10^2	$2^+_5-20\%$ $2^+_6-2\%$	$[2^+_1\otimes4^+_1]_{2^+}-3\%$ $[2^+_1\otimes4^+_5]_{2^+}-4\%$ $[3^-_1\otimes3^-_1]_{2^+}-35\%$ $[3^-_1\otimes5^-_1]_{2^+}-6\%$	25%

TABLE III. The same as in Table II for states with angular momentum and parity equal to 3^- and 4^+. Only states for which the transition charge densities were extracted from experiment are given.

	Experiment		Theory				
λ^π_ν	E_x, MeV	B(Eλ), $e^2F^{2\lambda+2}$	E_x, MeV	B(Eλ), $e^2F^{2\lambda+2}$	Q^+ Comp.	Q^+Q^+ Comp.	$Q^+Q^+Q^+$ Comp.
3^-_1	1.510	2.56×10^5	1.265	1.4×10^5	$3^-_1-56\%$ $3^-_2-2\%$	$[2^+_1\otimes3^-_1]_{3^-}-26\%$ $[2^+_1\otimes5^-_1]_{3^-}-5\%$	7%
3^-_2	2.779	4.46×10^4	2.787	2.6×10^4	$3^-_1-12\%$	$[2^+_1\otimes3^-_1]_{3^-}-36\%$ $[2^+_1\otimes5^-_1]_{3^-}-22\%$	27%
3^-_3	2.839	0.46×10^4	3.252	3.0×10^3	$3^-_1-5\%$ $3^-_2-7\%$	$[2^+_1\otimes5^-_1]_{3^-}-20\%$ $[3^-_1\otimes4^+_1]_{3^-}-39\%$	26%
3^-_4	2.967	8.1×10^3	3.359	4.1×10^4	$3^-_1-13\%$ $3^-_2-33\%$	$[2^+_1\otimes3^-_3]_{3^-}-3\%$ $[2^+_2\otimes3^-_1]_{3^-}-2\%$ $[2^+_1\otimes5^-_1]_{3^-}-6\%$ $[3^-_1\otimes4^+_3]_{3^-}-25\%$	15%
4^+_1	1.315	1.93×10^6	1.368	1.6×10^6	$4^+_1-40\%$ $4^+_2-2\%$	$[2^+_1\otimes2^+_1]_{4^+}-42\%$	12%
4^+_2	2.109	3.14×10^6	2.039	2.1×10^6	$4^+_1-45\%$ $4^+_2-5\%$	$[2^+_1\otimes2^+_1]_{4^+}-29\%$	12%
4^+_3			2.207	2.4×10^5	$4^+_1-3\%$ $4^+_2-84\%$	$[2^+_1\otimes2^+_1]_{4^+}-2\%$ $[2^+_1\otimes4^+_1]_{4^+}-4\%$	2%
4^+_4	2.451	1.13×10^6	2.449	4.9×10^5	$4^+_3-96\%$		
4^+_8	2.986	6.9×10^5	3.256	6.5×10^5	$4^+_5-43\%$	$[2^+_1\otimes2^+_5]_{4^+}-2\%$ $[2^+_1\otimes6^+_1]_{4^+}-8\%$ $[2^+_1\otimes6^+_4]_{4^+}-2\%$ $[3^-_1\otimes3^-_1]_{4^+}-22\%$ $[3^-_1\otimes5^-_1]_{4^+}-2\%$	14%

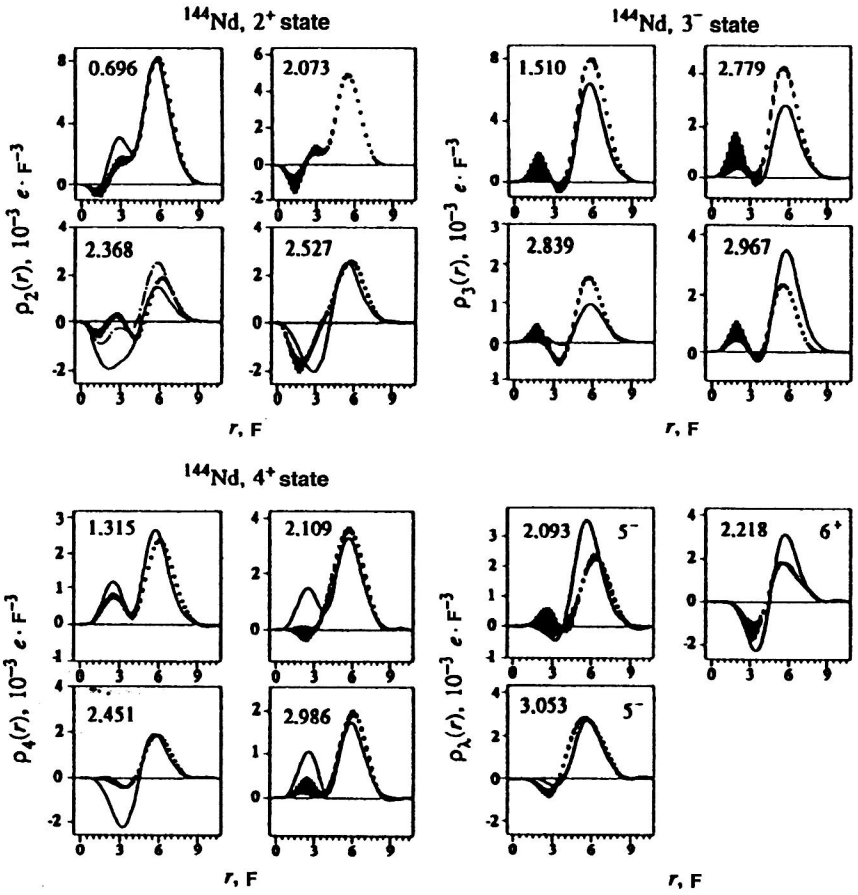

FIG. 2. The same as in Fig. 1 for excited states in ^{144}Nd. See the text for details.

of two-quasiparticle densities. We note that the $2^+_{3,4,7,8}$ one-phonon states are constructed almost only from proton two-quasiparticle configurations, and the others also contain a significant contribution of neutron components. This indicates that the two valence neutrons outside the closed $N=82$ shell are important.

The spectra of low-lying 2^+ states calculated using the wave function containing one-, two-, and three-phonon components are given in Table II along with the experimental data. In this table we have restricted ourselves to only excited states whose transition densities were extracted from data on the (e,e') reaction. The analogous results for 3^- and 4^+ states are given in Table III.

In our calculations the 2^+_1 state consists primarily of the lowest one-phonon 2^+ configuration (78%) with admixtures of two- (14%) and three-phonon (2%) components. The 2^+_2 state of energy 1.575 MeV is mainly the 2^+ component of the two-phonon multiplet $[2^+_1 \otimes 2^+_1]$ with an admixture of one- and three-phonon configurations. This state has not been seen in electron inelastic scattering owing to the small value of B(E2) for the transition. However, it is known from the data on (p,p') and (d,d') reactions. The behavior of the form factors suggests that in these reactions this excitation is a two-stage process occurring via the 2^+_1 level. This indicates that the two-phonon component makes a large contribution to the structure of this state, as predicted by our calculations.

The contribution of two-phonon configurations to the wave functions of low-lying 2^+ states in ^{144}Nd exceeds 10%, except in the case of the practically one-phonon 2^+_4, 2^+_5, and 2^+_9 states. For many low-lying 2^+ states the contribution of three-phonon configurations is also large ($\geq 10\%$). This is much different from the case of the low-lying 2^+ states in ^{142}Nd discussed above, where the contribution of two-phonon configurations is only a few percent, and the admixture of three-phonon components is negligible. This is a direct consequence of the enhanced coupling of phonon configurations with different numbers of phonons due to the two additional neutrons outside the closed shell. This results in stronger mixing, the splitting of different configurations, and decreased energy of the quadrupole excitations.

The experimental transition densities have been extracted for four 2^+ states in ^{144}Nd. They are shown in Fig. 2 along with the calculated ones. Our calculations predict nine states with given angular momentum and parity and excitation energy below 4 MeV, which is the same as the number of 2^+ states found in the (p,p') and (d,d') reactions in this energy range. The shape of the transition density of the 2^+_1 state of energy 0.696 MeV is reproduced well by the calculation, although the amplitude of the inner peak is slightly overestimated. The shapes of the transition densities for the levels at 0.696 and 2.073 MeV are very similar and coincide with the calculated density for the 2^+_1 state. This suggests that the 2^+_3 level arises as a result of the splitting of the lowest one-phonon configuration and is not seen in the calculation owing to the cutoff of the basis configurations.

The 2^+_4 and 2^+_5 states discovered in inelastic electron scattering at $E_x=2.368$ and 2.527 MeV agree fairly well in excitation energy and value of B(E2) with the corresponding

states in our calculations. However, this cannot be said of the shape of the transition densities. Whereas the experimental transition density of the state at 2.527 MeV is reproduced fairly well by the calculated density of the 2_4^+ state, the transition density of the state at 2.368 MeV corresponds somewhat with the calculated densities of only the states at about 700 keV higher (here we mean the 2_7^+ and 2_8^+ states in our calculations, whose transition densities are shown in Fig. 2 by the solid and dot-dash lines, respectively). In the calculation the 2_7^+ and 2_8^+ states arise as a result of fragmentation of the fifth one-phonon component (the most strongly collective after the lowest component) owing to the interaction with two-phonon configurations (mainly with $[3_1^- \otimes 5_1^-]_{2^+}$). The extension of the phonon basis relative to that used in the present calculation has a stronger affect on the properties of states containing collective phonons, which interact more strongly with complex configurations. It is quite possible that this leads to splitting of the fifth one-phonon configuration and decrease of the excitation energy, which approaches the energy of the 2_4^+ state seen experimentally.

For octupole excitations in ^{144}Nd we have only two one-phonon configurations below 4 MeV. The first is collective with $B(E3)=2.3\times10^5\ e^2F^6$ and has excitation energy 2.350 MeV. The second is predominantly a two-quasiparticle configuration with $E_x=3.369$ MeV and $B(E3)=9.8\times10^2\ e^2F^6$. When the interaction with complex configurations is included, the number of octupole states below 4 MeV increases to five. The calculated and experimental [from the (e,e') reaction] values of the location and B(E3) for octupole states are given in Table III. The mixing of one-, two-, and three-phonon configurations in the wave functions of 3^- states is significant. For the lowest 3^- state the one-phonon component is dominant (56%), but the wave function of even this state contains admixtures of 31% from two-phonon and 7% from three-phonon configurations. The dominant contribution to the structure of all the other 3^- states comes from two-phonon configurations (up to 60% in the case of 3_2^- and 3_3^-) with a large admixture, more than 15%, of three-phonon ones.

Four 3^- states in ^{144}Nd were discovered experimentally in inelastic electron scattering. Their transition charge densities are shown in Fig. 2. The transition densities of all these states are similar in shape, but have different amplitudes. This is quite natural in view of the fact that the shape of the transition densities of these states is, as shown by our calculations, determined only by the shape of the lowest one-phonon 3^- configuration, while the amplitude is proportional to the contribution of this configuration to the wave function of each state.

As for states of other multipole orders, the experimental distribution of the strength of hexadecapole transitions in ^{144}Nd is reproduced quite well by our calculation (see Table III). The experimental transition charge densities of the 4^+ states in this nucleus are shown in Fig. 2. The shape of the transition densities of the levels found at excitation energy 1.305, 2.109, and 2.451 MeV agree well with the densities for the predicted 4_1^+, 4_2^+, and 4_4^+ states, respectively. The principal component of the first two is the lowest one-phonon configuration, which contributes 40% and 45%, respectively. The strength of this configuration is split mainly owing to the interaction with the two-phonon configuration $[2_1^+ \otimes 2_1^+]_{4^+}$. In ^{142}Nd the two-phonon configuration of lowest energy, $[2_1^+ \otimes 2_1^+]_{4^+}$, lies considerably higher than the lowest one-phonon 4^+ configuration. As a result, the lowest 4^+ state is practically a one-phonon state, and the two-phonon configuration mixes mainly with the fourth one-phonon configuration close to it in energy, forming the 4_4^+ and 4_5^+ states. Owing to the considerable decrease of the energy of the lowest one-phonon 2^+ configuration, in ^{144}Nd the two-phonon configuration $[2_1^+ \otimes 2_1^+]_{4^+}$ lies near the one-phonon 4_1^+ configuration, and mixing with it gives rise to the 4_1^+ and 4_2^+ states with similar shapes of the transition charge density.

The transition density of the level at 2.451 MeV corresponds well with the density of the 4_4^+ state, consisting primarily of the noncollective third one-phonon configuration. The 4_3^+ state most likely was simply not observed experimentally owing to its small value of B(E4). Judging from the shape of its transition density, the level at 2.986 MeV corresponds to the eighth 4^+ state in our calculations. Taking into account the fact that in experiments on proton and deuteron inelastic scattering, which are able to isolate weaker states, seven (or eight) 4^+ states with energy below 3.7 MeV have been discovered in ^{144}Nd, this correspondence seems quite reasonable.

The transition densities of the two 5^- and one 6^+ level found in ^{144}Nd in the (e,e') reaction are also shown in Fig. 2. The first 5^- level at 2.093 MeV has a surface peak in the transition density, indicating its collective nature, while the peak of the second level at 3.053 MeV is shifted by about 1 F inside the nucleus. Our calculations predict six 5^- states with energy below 4 MeV. The shape of the transition densities of the 5_1^-, 5_2^-, and 5_3^- states is mainly determined by the density of the lowest one-phonon configuration, which is strongly fragmented among these states as a result of interaction with the $[2_1^+ \otimes 3_1^-]_{5^-}$, $[2_1^+ \otimes 5_1^-]_{5^-}$, and $[3_1^- \otimes 4_1^+]_{5^-}$ configurations. The shift of the maximum of the transition density of the second state inside the nucleus is associated with the destructive admixture of the second one-phonon configuration in the wave function of this state. The only 6^+ level seen in inelastic electron scattering corresponds to the second 6^+ state in our calculations. The 6_1^+ state at 1.822 MeV corresponds to the 6_1^+ level at 1.791 MeV seen in inelastic proton and deuteron scattering.[15]

The main difficulties in describing transitional nuclei, for example, the isotope ^{146}Nd, in our approach are associated with the very strong interaction between different one-, two-, and three-phonon configurations. The strong coupling of different configurations makes it necessary to take as many of them as possible into account in the calculations. This leads to problems of a purely computational nature. Therefore, in the calculations for transitional nuclei we had to cut off the phonon basis used in constructing the excited-state wave functions much more strongly than in the calculations discussed above. In cutting off the basis, we tried to use all the principal configurations which could contribute noticeably to the structure of states with excitation energy below 3 MeV. As a result, when studying ^{146}Nd (Ref. 9) we included di-

TABLE IV. Excitation energies and reduced transition probabilities B(Eλ) in ^{146}Nd.

Experiment		Theory		Experiment		Theory	
E_x, MeV	B(Eλ), $e^2F^{2\lambda+2}$	E_x, MeV	B(Eλ), $e^2F^{2\lambda+2}$	E_x, MeV	B(Eλ), $e^2F^{2\lambda+2}$	E_x, MeV	B(Eλ), $e^2F^{2\lambda+2}$
	2^+ State				4^+ State		
0.453	6.91×10^3	0.565	5.44×10^3	1.044	1.50×10^6	0.870	1.42×10^6
1.303		1.640	2.42×10^1	1.747	3.61×10^6	1.590	2.33×10^6
1.470	6.8×10^2	2.150	1.06×10^3	1.919			
1.789		2.369	1.84×10^1	1.987	2.1×10^6	2.040	2.19×10^6
		2.490	2.66×10^{-2}			2.340	1.64×10^5
1.977	2×10^2	2.600	2.08×10^2	2.622	3×10^5	2.450	1.98×10^5
2.198		2.980	1.82×10^2	2.935	1.6×10^6	2.520	1.83×10^5
2.665	1.68×10^2	3.380	9.77×10^1			2.580	1.15×10^5
2.976	6×10^1	3.430	2.80×10^2			3.010	1.29×10^6
	3^- State				5^- State		
1.190	3.52×10^5	1.150	1.62×10^5	1.517	2.64×10^8	1.670	1.91×10^8
2.339	5.1×10^4	2.380	5.34×10^4	2.570	8.5×10^7	2.520	5.25×10^7
2.530	2×10^4	3.010	4.92×10^2	2.748	2.93×10^7	3.120	4.52×10^7
2.690	5×10^3	3.180	6.26×10^3	2.877		3.170	1.39×10^7
2.807		3.390	3.71×10^4	2.915	4.7×10^7	3.510	1.97×10^7
2.822		3.840	1.05×10^4	3.000	2.7×10^7	3.810	1.83×10^7
2.850	2×10^4						

rectly in the calculations all one-phonon configurations with $E_x \leq 4.0$ MeV, which make up most of the multipole strength in the energy range in question, and also largely determine the shape of the transition charge densities of excited states. We also included two-phonon configurations with $E_x \leq 5.5(6.0)$ MeV, which determine the fragmentation of one-phonon configurations among low-lying states. Three-phonon configurations constructed from the lowest collective 2^+, 3^-, 4^+, and 5^- one-phonon configurations were also included. This cutoff of the phonon space obviously leads to restrictions on the applicability of the calculations to nuclei with strong configuration coupling, especially for states with high excitation energy. This results in the loss of some of the weak states and underestimation of the total number of excited states of various multipole orders. However, in inelastic electron scattering it is mainly levels with a significant contribution from one-phonon configurations which are excited, and so the restrictions we impose appear reasonable in describing the experimental data obtained in (e,e') reactions.

The relatively simple picture of the structure of nuclear excitations in terms of one- and multiphonon configurations for the semimagic isotope ^{142}Nd is greatly changed in the case of the transitional nucleus ^{146}Nd. The strong coupling of different configurations leads to significant fragmentation of the strength of the one-phonon components among a large number of excited states, and as a result practically all the states in the transitional nuclei considered below have a very complicated structure. We shall therefore discuss only the main features when comparing the results of our calculations with the experimental data, and shall omit discussion of the calculations performed in the one-phonon approximation.

In Table IV we give the results of our calculations of the spectrum and reduced excitation probabilities B(Eλ) for states with angular momentum and parity 2^+, 3^-, 4^+, and 5^- in ^{146}Nd. For comparison, here we also give the experimental data obtained from inelastic electron scattering. The transition charge densities of excited states extracted from the form factors of this reaction are shown in Fig. 3 along with the calculated ones.

The experimental distribution of the strength of the 2^+ states in ^{146}Nd is reproduced well in our calculation. The theory predicts the existence of three strong 2^+ states, namely, 2_1^+, 2_3^+, and 2_6^+, and three weak states, which are extremely difficult to find in the (e,e') reaction. Comparison of the experimental and calculated transition densities of the 2_1^+ state indicates that the deformation effect is present in the ^{146}Nd isotope. Although the shape of the transition density is reproduced well by the calculation, except for a slight overestimation of the amplitude of the inner peak (the reason for which we know), the maximum of the surface peak in the experimental transition density is shifted by 0.15 F compared to the calculated one. The description of the transition density of the 2_3^+ level is also good. The main contribution to the structure of this state comes from the two-phonon $[2_1^+ \otimes 4_1^+]_{2^+}$ configuration, which is shifted to lower energies as a result of interaction with three-phonon configurations. The contribution of the two-phonon transition density inside the nucleus is suppressed owing to destructive interference with the other components, and the small admixtures from the collective first and second one-phonon components give the dominant contribution to the shape of the density.

The transition density of the 2_6^+ level was not extracted from the data on (e,e') scattering owing to the nearby 4^+ level, because its form factor was isolated only for the four lowest values of the momentum transfer. However, comparison with experiment at the form-factor level indicates good agreement between the calculation and the experimental

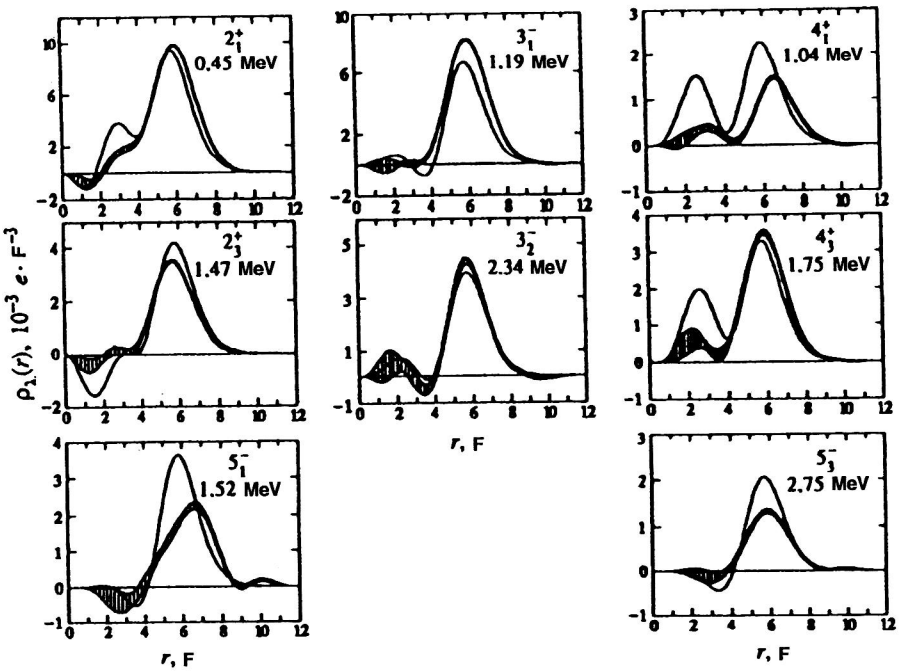

FIG. 3. The same as in Fig. 1 for excited states in ^{146}Nd.

data. On the whole, the description of the quadrupole states up to about 2 MeV is quite satisfactory. Although some indications of the presence of deformation are seen in the behavior of the transition density of the 2_1^+ level, the other quadrupole states, in particular, the 2_6^+ level, correspond to a purely vibrational picture of the excitation. The slight overestimation of the energies of higher states is of about the same magnitude as in the case of the semimagic ^{142}Nd nucleus.

For octupole states, the transition densities of only the two levels at 1.190 and 2.339 MeV were extracted from the form factors of (e,e') scattering. These two densities, shown in Fig. 3, are very similar in shape. We have already encountered a similar situation when studying 3^- states in ^{144}Nd. Here the reason is the same, namely, the presence of a single collective 3_1^- one-phonon configuration at low energies, the admixture of which is decisive for the resulting transition densities of the 3^- levels. In particular, for the 3_1^- and 3_2^- states this configuration mixes most strongly with the two-phonon configuration $[2_1^+\otimes 3_1^-]_{3^-}$. Our calculation predicts only six 3^- states with energy below 4 MeV, which is considerably fewer than seen in experiment. The same underestimation of the number of states by the calculation also occurs for ^{144}Nd. One explanation might be that the calculations should be extended to energies above 4 MeV for nuclei with a nonclosed shell. Another might be the cutoff of multiphonon configurations in the direct calculation. In general, extension of the phonon basis should push simple configurations to lower energies. This tends to increase the number of octupole states in the energy range under study. On the other hand, this should not strongly change the structure of the lowest octupole states, because we have taken into account all the possible configurations in the region where they are localized.

The hexadecapole states in ^{146}Nd possess some curious features. First, the transition charge density of the 4_1^+ level has a maximum at an even larger value of r than the density of the 2_1^+ level. This again indicates that this nucleus has a positive hexadecapole moment, in agreement with the result of the calculations of Ref. 16, which predict $\beta_4=0.056$ for this nucleus. Second, the transition density of the 4_2^+ level has a shape similar to that of the 4_1^+ level, but its maximum is shifted inside the nucleus by 0.7 F. Third, the hexadecapole strength of the 4_2^+ level is more than two times larger than that of the 4_1^+ level. Since our calculational scheme does not take into account the deformation of the nuclear surface, we cannot attempt to explain the first two effects. Regarding the third, the calculation also predicts a large value of B(E4) for the second 4^+ state compared to the first. The reason lies in the structure of these states. As a result of the interaction with three-phonon configurations, the pole of the two-phonon configuration $[2_1^+\otimes 2_1^+]_{4^+}$ is strongly shifted from 3.75 MeV to 1.04 MeV, i.e., below the energy of the lowest 4^+ one-phonon configuration, 2.030 MeV. Consequently, the 4_1^+ state consists of 50% two-phonon configurations and 30% three-phonon ones, despite the low excitation energy of this state. On the other hand, the 4_2^+ state is characterized by a contribution of 20% from the lowest one-phonon configuration, 45% from $[2_1^+\otimes 4_1^+]_{4^+}$ (also shifted from 3.46 to 1.81 MeV), and 20% from three-phonon configurations. The bulk of the strength of the lowest one-phonon configuration is concentrated at the third 4^+ state. This third 4^+ state can be associated with the level at 1.987 MeV. The transition density for this level was not extracted from the reaction form factor owing to the admixture of the nearby 2_6^+ level, but comparison of the experimental form factor with the form factor calculated using the transition density of the 4_3^+ state completely favors this association.

The experimental transition charge density has been obtained for two states with angular momentum and parity 5^-. The first, at energy 1.517 MeV, has a maximum at very large

r, as in the case of the lowest hexadecapole state. The density of the state at 2.748 MeV has a surface maximum at a value of r corresponding to the spherical picture of the nucleus. The structure of the calculated 5^- states is very complex. The lowest one-phonon 5^- configuration is practically evenly distributed between the 5_1^-, 5_2^-, 5_3^-, and 5_5^- states. In addition, each state contains roughly 50% two-phonon and 20% three-phonon components. The only exception is the 5_4^- state, which is a practically pure second one-phonon configuration. The theoretical description of the 5^- states is obviously very sensitive to the choice of basis of the one- and multiphonon configurations, and therefore serves as a good test of the applicability of the configurational space which is used. The agreement with experiment regarding the distribution of the E5 transition strength among low-lying 5^- states is completely satisfactory. The presence of a relatively strong low-lying 5^- state and several weaker states of high excitation energy with roughly equal values of B(E5) is reproduced by the calculation. The shape of the transition density for the experimental level at 2.748 MeV is also reproduced well.

On the whole, we have shown that microscopic calculations based on a spherically symmetric mean field can be used with few constraints to calculate the properties of low-lying states in transitional nuclei. The structure of practically all the excited states is found to be very complicated, and the transition densities of some states indicate that deformation is present. However, the general features of the strength distribution of one-phonon configurations is reproduced reasonably well by the calculation when a sufficiently large basis of multiphonon configurations is used.

The transition charge densities of low-lying excitations have also been calculated using the QPM for the nuclei ^{118}Sn (Ref. 17), ^{140}Ce (Ref. 18), ^{142}Ce (Ref. 19), and ^{196}Pt (Ref. 20), in addition to the chain of neodymium isotopes. The calculations for these nuclei also show that the model gives a good quantitative description of the available experimental data. The structure and electromagnetic properties of low-lying states in other semimagic nuclei of mass $A \sim 140$ have been studied using the QPM with the wave function (7) also in Ref. 21.

3. THE STRENGTH DISTRIBUTION OF ISOSCALAR $E\lambda$ TRANSITIONS

The experimental data obtained in proton and deuteron inelastic scattering are in some sense auxiliary to the data extracted from electron inelastic scattering. High-resolution studies of the (e,e') reaction have shown that the Eλ-transition strength in intermediate and heavy nuclei is significantly fragmented. Accordingly, detailed information about weak states, i.e., states characterized by a small value of B(Eλ), cannot be obtained from the (e,e') data owing to the radiative tail of the ground state and nearby collective levels. However, nuclear reactions involving hadronic particles (particles interacting with the target via nuclear forces) and leading to nuclear excitations of the order of several MeV, where the experimental spectra are sets of discrete lines, are not susceptible to the influence of the ground state arising from various physical processes. Therefore, data on the strength distributions of E3 and E4 transitions have mainly been obtained from the scattering of hadronic particles, and particularly from the (p,p') reaction.[22–24] On the other hand, since the nuclear interaction between the beam particles and the target includes components pertaining to the proton and neutron systems of the nucleus, reactions involving hadrons supplement the data obtained in (e,e') reactions with information about the neutron component of nuclear excited states.

In this section we shall compare the strength distributions B(Eλ) of transitions in the neodymium isotope chain ^{142,144,146}Nd calculated in the QPM, using the same excited-state wave functions as in the preceding section to calculate the transition charge densities, with the experimental data. The data were obtained at the KVI cyclotron (Groningen) in the inelastic scattering of protons and deuterons at various angles and energies 30.5 and 50.6 MeV, respectively. Energy resolutions of 12–15 keV in (p,p') and 15–22 keV in (d,d') reactions were attained in these experiments. The spin and parity of the excited states were determined by comparing the momentum-transfer dependence of the cross section with the calculations using the coupled-channel method performed for various momentum transfers λ.

The calculated strength distributions of the reduced isoscalar-transition probability as a function of excitation energy in the nuclei ^{142,144,146}Nd for states of various multipole orders are shown in Fig. 4. There we also show the experimental data from inelastic proton and deuteron scattering. The experimental results are shown as points, and the theoretical results are shown by the vertical dashed lines. To better appreciate the correspondence of the gross structure in the transition-strength distribution, both the experimental and the theoretical data are also presented in the form of strength functions obtained using a Gaussian of width 200 keV as the profile function. Since we have discussed the structure of the low-lying excited states in these isotopes in detail in the preceding section, here we restrict ourselves to only comments of a general nature regarding the agreement between the theoretical predictions and the experimental data. For the ^{144,146}Nd isotopes the calculations were performed using the interacting-boson model[25] (IBM-1) in addition to the QPM. When discussing the results we shall also consider the general regularities and differences in the predictions of these two nuclear models, which include the interaction of one- and multiphonon configurations.

The most clearly expressed peaks in the energy spectra correspond to the excitation of 2^+, 3^-, and 4^+ states. Most of the E2 strength is concentrated on the 2_1^+ state with B_S(E2) increasing from 20 Weisskopf units in ^{142}Nd to 43 W.u. in ^{146}Nd. The mass dependence of the results is much weaker in the sense of exhausting the energy-weighted sum rules (EWSRs). In fact, the 2_1^+ state in all the isotopes accounts for 6–7% of the EWSRs, and all the other 2^+ states below some fixed excitation energy E_Σ account for 4–5%. To construct a systematics for different isotopes at an equivalent energy level, we took E_Σ to be $E(3_1^-)$ +2.1 MeV.

The distribution of the E3-transition strength is also

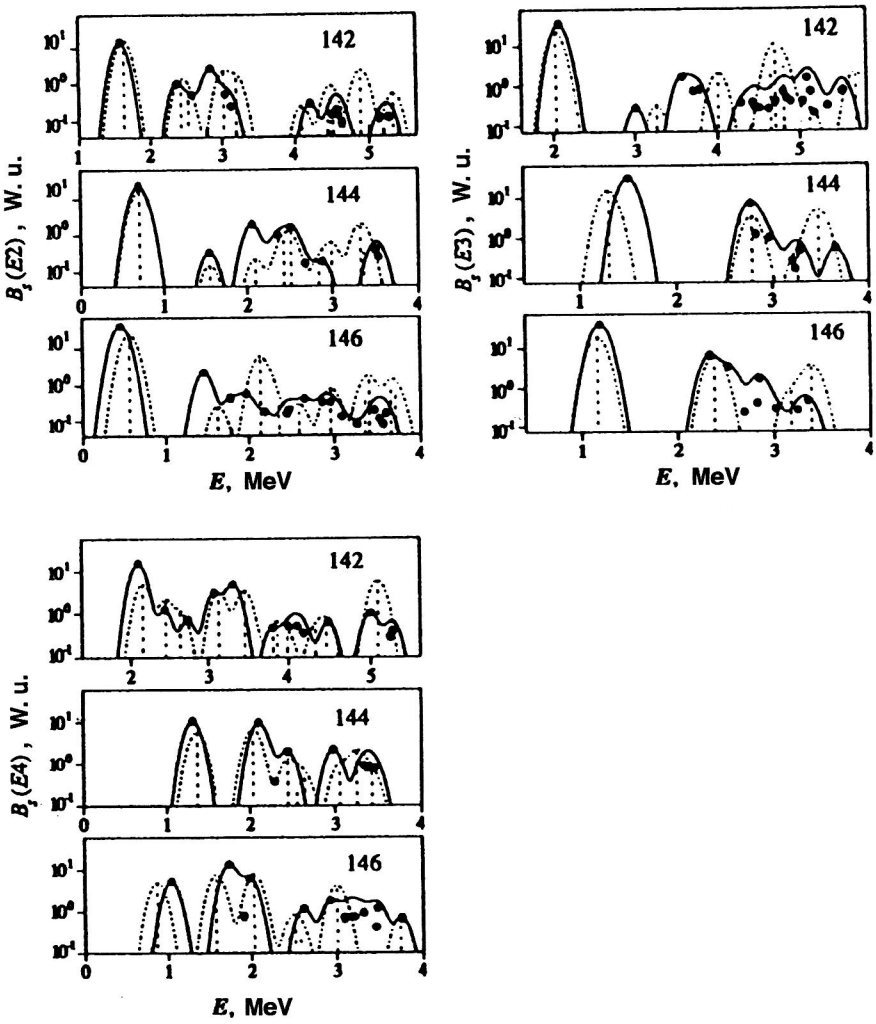

FIG. 4. Strength distribution of isoscalar $E\lambda$ transitions in neodymium isotopes ^{142,144,146}Nd in Weisskopf units. The experimental results are shown as points and solid lines, and the theoretical ones as dashed lines. See the text for details.

dominated by the lowest 3^- state with transition probability ranging from 34 W.u. in ^{142}Nd to 42 W.u. in ^{146}Nd. The percent contributed to the EWSRs by the lowest 3^-_1 state decreases from 7% in ^{142}Nd to 5% in ^{146}Nd, and for the other 3^- states below E_Σ it rises from 1.2 to 3%. This behavior confirms the results of earlier studies: as the number of valence particles grows, the low-lying states become more strongly collective, and a significant part of the octupole strength is transferred from the lowest state to the next highest 3^- states. This strength redistribution occurs only among the 3^-_1 and neighboring octupole states, and does not affect higher states like, for example, the low-energy octupole resonance. Theoretical calculations give a simple interpretation of this phenomenon: the distribution of the E3-transition strength at low excitation energies is fully explained by the fragmentation of the lowest 3^- phonon or f boson in the IBM.

The distribution of the E4-transition strength has a much more complicated structure. In ^{142}Nd the 4^+_1 state has the largest value of B(E4), while in ^{144}Nd the value of B(E4) for the 4^+_1 state is comparable to that for the second and third 4^+ states. In ^{146}Nd the lowest 4^+ state is already two times weaker than the next state. This behavior is related to the evolution in the interaction of the one- and two-phonon components in the wave function of the 4^+ states. The 4^+ levels are very highly fragmented; in all the nuclei the number of states with a given spin and parity is very large, which fully corresponds to the theoretical predictions. The total E4-transition strength below E_Σ makes up about 2% of the EWSRs.

The experimental strength distribution of isoscalar transitions in ^{142}Nd and ^{144}Nd agrees well with the theoretical predictions. The agreement for ^{146}Nd is somewhat worse, but still acceptable. It is worse because of the difficulties associated with the enhanced interaction between the one-, two-, and three-phonon configurations of the wave function in approaching the region of transitional nuclei. This problem has already been discussed in the preceding section.

The IBM reproduces the strengths of only the first and second excited 2^+ states well, and significantly underestimates the strengths of higher-lying states. This is not surprising, because, as the QPM calculations show, at energies above 2 MeV one-phonon configurations different from the 2^+_1 one are responsible for the E2-transition strength. For the IBM this is equivalent to the need to introduce additional d bosons.

The number of 3^- states with significant E3-transition strength is slightly lower than in experiment, but the gross structure of the distribution is reproduced well by the calculations. The most serious defects of the calculation appear in

the case of the lowest 3^- state, the strength of which is systematically underestimated, this underestimate becoming worse in moving along the isotope chain. The reason for this is the following. The closed N=82 shell affects E3 transitions most strongly, since such transitions are forbidden inside the subshell by spin–parity considerations. This problem cannot be eliminated by a simple change of the model parameters used in the calculation. Actually, we can use the parameters to enhance the collective nature of the lowest one-phonon 3^- configuration and thereby improve the agreement with the experimental data on the E3-transition strength, but this causes the lowest 2^+ and 4^+ states to have too low an excitation energy. This effect is the result of the interaction of the 2_1^+ one-phonon configuration with the two-phonon configuration $[3_1^-\otimes 3_1^-]_{2^+}$. The matrix element of this interaction in neodymium isotopes is very large and strongly depends on how collective both the one- and the two-phonon configurations are. The same occurs for the 4_1^+ state.

For 3^- excited states our calculations and the IBM give more or less equally good descriptions, which is easily explained. The IBM-1-*sdf* describes low-lying 3^- states as the fragmentation of the strength of a single f boson with an admixture of df or $sd\cdot sf$ configurations. Similarly, the QPM describes the same states as the fragmentation of the lowest 3^- one-phonon component as a result of mixing with the two-phonon components $[2_1^+\otimes 3_1^-]_{3^-}$, $[2_1^+\otimes 5_1^-]_{3^-}$, $[3_1^-\otimes 4_1^+]_{3^-}$, $[3_1^-\otimes 6_1^+]_{3^-}$, and so on.

Comparison of the theoretical QPM and the IBM calculations with the experimental data for the E4-transition strength distribution gives results similar to those for the strength distribution of quadrupole transitions. The IBM-1-*sdg* reproduces the strength of low-lying 4^+ states, but strongly underestimates it for energies above 2.2 MeV. On the whole, the agreement of the QPM results with the experimental data is significantly better. In our calculations the E4-transition strength distribution is due to the lowest six 4^+ one-phonon configurations. This again indicates the need to introduce additional bosons with higher excitation energy than the d and g bosons.

4. LOW-LYING 1^- STATES AND E1 TRANSITIONS BETWEEN LOW-LYING STATES

4.1. Low-lying 1^- states in spherical nuclei

The properties of low-lying dipole states in spherical nuclei differ fundamentally from those of low-lying states of other multipole orders. This is because, in contrast to states with $\lambda\geqslant 2$, there is no collective low-lying one-phonon 1^- state which largely determines the properties of the strength distribution of electromagnetic transitions of this multipole order at low excitation energies. More precisely, there is such a state, but it is a ghost state corresponding to motion of the nucleus as a whole, and a large number of studies have been devoted to the problem of correctly including it (see, for example, Ref. 26). As a result, the first one-phonon 1^- states appear in the calculations at energies above 5 MeV and are of practically pure two-quasiparticle nature. On the other hand, two-phonon states constructed from one-phonon 2_1^+ and 3_1^- configurations appear in the energy spectra at lower excitation energies, especially in nuclei with an open shell, in which the energies of the first 2^+ and 3^- levels are greatly lowered. However, the probability of exciting collective two-phonon states $[2_1^+\otimes 3_1^-]_{1^-}$ in nuclear processes is greatly suppressed owing to the single-particle nature of the transition operator. In fact, a direct transition to a two-phonon or 2p2h configuration via the single-particle operator of the external field is of next order in smallness compared to a transition to a one-phonon or 1p1h configuration. Such a transition is completely forbidden in models in which excited states are treated in the language of ideal bosons. When the fermionic structure of the phonons is taken into account, as in the QPM, the direct transition g.s.$\rightarrow[2_1^+\otimes 3_1^-]_{1^-}$ becomes allowed owing to ground-state correlations, but, of course, it is strongly suppressed.[27] The two-stage excitation of $[2_1^+\otimes 3_1^-]_{1^-}$ states is even weaker, since it includes the matrix element of the E3 transition.

Therefore, electric dipole transitions at low excitation energies are a special tool for studying nuclear structure. In studying these we encounter the problem of the very sensitive balance between, on the one hand, the weak matrix elements of the main components of the wave function and, on the other, the strong matrix elements of E1 transitions to the weakly admixed one-phonon configurations belonging to the giant dipole resonance. However, despite the small values of the reduced transition probability B(E1,g.s.$\rightarrow[2_1^+\otimes 3_1^-]_{1^-}$), low-lying 1^- states were discovered long ago (see, for example, Refs. 28–30), and the structure of these states was successfully interpreted as being of a two-phonon nature.[27,31,32] However, only the appearance of modern, highly efficient Ge detectors has made it possible to experimentally detect 1^- states at higher excitation energies.

The first data on the distribution of the E1-transition strength among low-lying 1^- states were obtained for the semimagic isotope ^{140}Ce in photon resonance scattering.[33] The energy range from 4.8 to 8.9 MeV in ^{140}Ce had been studied earlier in tagged-photon experiments.[34] However, owing to the limits on the energy resolution, individual states were not distinguished in this early experiment; only the gross structures in the photoabsorption cross section, referred to as pygmy resonances, were seen. The properties of pygmy resonances have been studied using the QPM to calculate the E1-transition strength function in this energy range, with the 1^- states described by a wave function containing one- and two-phonon components.[35] Of course, the strength-function method cannot be used to obtain information about the structure of the states forming these resonances.

The experiment was performed using bremsstrahlung gamma quanta obtained at the S-DALINAC linear accelerator in Darmstadt. Excitation energies up to about 6.7 MeV were studied. The experimental transition strength distribution B(E1) for ^{140}Ce is shown in Fig. 5a. It should be noted that in this experiment it was not possible to determine the parity of a transition but only the spin, and so the distribution shown in Fig. 5a was obtained assuming that all the excited states are 1^- states. The probability that some of them are 1^+ states will be discussed below.

The experiment recorded the 1_1^- state known earlier at

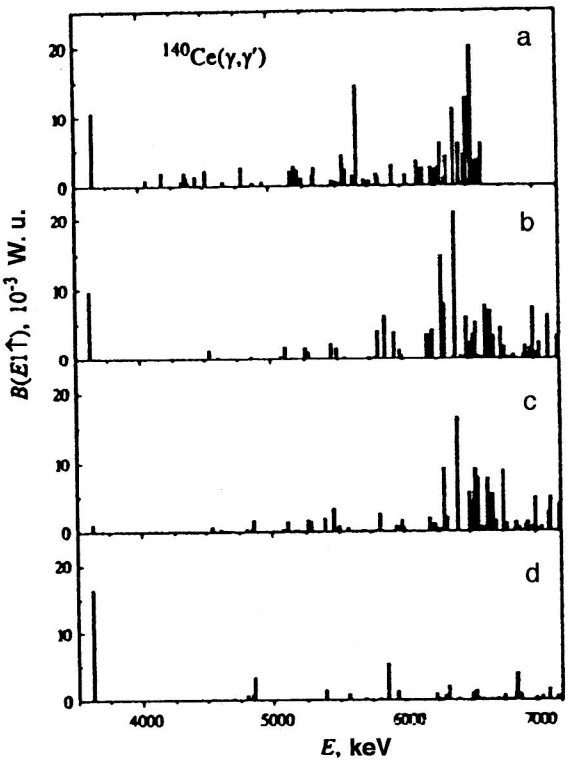

FIG. 5. (a) Experimental E1-transition strength distribution. (b)–(d) Results of the calculation using the wave function containing one-, two-, and three-phonon configurations; (c) is the one-phonon part and (d) is the two-phonon part of the E1 transitions. In this calculation, three-phonon configurations are mainly responsible for fragmentation.

3.643 MeV, which is the 1^- component of the two-phonon multiplet $[2_1^+\otimes 3_1^-]$ with $B(E1;0^+\to 1^-)=(18.2\pm 2.2)\times 10^{-3}\ e^2F^2$. The 1^- state at 5.66 MeV, also known earlier,[36,37] was also recorded. Using the known ratio $\Gamma_0/\Gamma=0.95(5)$ from Ref. 36, an unexpectedly large E1-transition strength with $B(E1;0^+\to 1^-)=(24.8\pm 4.9)\times 10^{-3}\ e^2F^2$ was found for this state. In addition, a large number of weaker transitions (52 altogether) to states which were not known before were discovered.

To analyze the experimental E1-transition strength distribution, we performed calculations using the wave function (7) containing one-, two-, and three-phonon components. We calculated the excited-state wave functions and transition probabilities $B(E1;0^+\to 1^-)$ and $B(M1;0^+\to 1^+)$ in ^{140}Ce. All one-phonon 1^- configurations up to 20 MeV were included. The effect of the dipole resonance on low-lying E1 transitions is usually referred to as the core dipole polarization effect[38] and is described by introducing effective charges of the $E1$ transitions. Since all the one-phonon states forming the giant dipole resonance are taken into account explicitly, there is no need to introduce the static polarizability χ in these calculations. The calculations included two- and three-phonon configurations formed from phonons of natural parity with $J^\pi=1^--6^+$ up to excitation energies of 9 MeV. Since the density of multiphonon configurations grows strongly with excitation energy, we excluded those configurations which do not play a significant role in the E1-transition strength distribution up to excitation energies of 7 MeV.

The results of the calculation are shown in Fig. 5b. The agreement with the experimental transition strength distribution B(E1) shown in Fig. 5a is quite good. We again note that in spherical nuclei there are no collective one-phonon 1^- configurations in the low-energy region. Therefore, there are three basic mechanisms which can explain the experimental E1-transition strength. The first is the effect of the giant dipole resonance. In phenomenological approaches this effect is described by extrapolating its low-energy tail. In microscopic theories it is treated in a natural manner as the result of coupling between one- and two-phonon configurations. Since the giant dipole resonance is located about 10 MeV above this energy range, only a very small part of its total strength is felt at energies of a few MeV. The second mechanism is the excitation of noncollective and weakly collectivized 1^- states having relatively small values of B(E1) but located in the region under study. The last mechanism is the direct excitation of two-phonon configurations from the ground state. Although the direct excitation of two-phonon configurations is an effect of next order in smallness compared to the excitation of one-phonon configurations, the excitation of some collective configurations, in particular, $[2_1^+\otimes 3_1^-]_{1^-}$, plays an important role, because the other two mechanisms also give small values of the E1-transition strength.

All these mechanisms for exciting 1^- states have been included in the calculation whose results are shown in Fig. 5b. The E1-transition operator consists of two terms corresponding to the excitation of one- and two-phonon components, respectively. The reduced probability of the direct electromagnetic excitation of two-phonon states $[\lambda_{i_1}^{\pi_1}\otimes\lambda_{i_2}^{\pi_2}]_{\lambda^\pi}$, consisting of an i_1 phonon of multipole order λ^{π_1} and an i_2 phonon of multipole order λ^{π_2}, from the nuclear ground state $|0^+_{\text{g.s.}}\rangle$ in our approach has the form

$$B(E\lambda;O^+_{\text{g.s.}}\to[\lambda_{i_1}^{\pi_1}\otimes\lambda_{i_2}^{\pi_2}]_{\lambda^\pi})=(2\lambda_1+1)(2\lambda_2+1)\times\left|\sum_{j_1j_2j_3\tau}e_\tau^{(\lambda)}f^\lambda_{j_1j_2}(\tau)v^{(-)}_{j_1j_2}\begin{Bmatrix}\lambda_2 & \lambda_1 & \lambda\\ j_1 & j_2 & j_3\end{Bmatrix}\times(\psi^{\lambda_2 i_2}_{j_2j_3}\varphi^{\lambda_1 i_1}_{j_3j_1}+\psi^{\lambda_1 i_1}_{j_3j_1}\varphi^{\lambda_2 i_2}_{j_2j_3})\right|^2. \quad (20)$$

The simplest method of calculating the matrix element of the transition from the ground state to the two-phonon state is to use the Marumori expansion[39] of the single-particle, fermionic, electromagnetic-transition operator $a^+_{jm}a_{j'm'}$ into an infinite sum of boson (phonon) operators.

To display the role of each of the mechanisms for exciting 1^- states and the result of their interference in different regions of the energy spectrum, in Fig. 5c we show the contribution of the one-phonon and in Fig. 5d the two-phonon component of the E1-transition operator to the complete E1 strength distribution over the set of the same states as in Fig. 5b.

The experimental values of the energy and excitation probability of the 1_1^- state in ^{140}Ce are reproduced well in the calculation. The interference between the one- and two-

phonon components of this state is destructive. The calculation indicates that the $[2_1^+\otimes 3_1^-]_{1^-}$ configuration contributes 85% to the wave function of this state.

The experimental E1-transition strength near 4.5 MeV is underestimated by the theory. The collective two-phonon configuration $[3_1^-\otimes 4_1^+]_{1^-}$ located roughly at this excitation energy has matrix element for excitation from the ground state much smaller than the $[2_1^+\otimes 3_1^-]_{1^-}$ configuration. On the other hand, the matrix element of the interaction with the one-phonon configurations forming the dipole resonance is not large enough to contribute significantly to its dipole strength.

At energies $E_x\approx 5.5-6.5$ MeV we observe significant constructive interference between the one- and two-phonon components, which practically doubles the transition strength B(E1) near 6 MeV compared to the purely one-phonon strength and is important for describing the experimental results.

We have also calculated the M1-transition strength distribution up to excitation energy 7.5 MeV. Most of the strength is associated with the direct excitation of two-phonon configurations. The total strength is $\Sigma B(M1;0_1^+\rightarrow 1^+)=0.87\mu_N^2$. If we rescale this strength to the cross section for photon inelastic scattering, the total B(M1) corresponds to less than 5% of the total experimental cross section, which gives an idea of the validity of the assumption that all states with unit spin found experimentally have negative parity.

4.2. The possibility of finding the 2^+ component of the two-phonon multiplet $[3_1^-\otimes 3_1^-]$ in reactions involving gamma quanta

The high efficiency of the new generation of germanium detectors demonstrated in the experiment on the E1-transition strength distribution in the low-lying region has made it possible to propose a new experiment to discover the 2^+ component of the two-phonon multiplet $[3_1^-\otimes 3_1^-]$ in ^{208}Pb using the (γ,γ') reaction.[40] The present subsection is devoted to this possibility. The search for two-phonon octupole states in the doubly magic ^{208}Pb nucleus is one of the most interesting problems in the physics of nuclear structure and has a rather long history. In spherical nuclei such as ^{208}Pb, collective excitations of the nuclear surface form the lowest excitation modes, which are well described in the phonon approach. In this approach there naturally arise multiplets of multiphonon states located at an energy equal to the sum of the energies of their phonon components. Study of the properties of such multiplets may answer the question of how well the harmonic picture applies to real nuclei. Moreover, the energy splitting of the multiplets makes it possible to study the role of effects due to the Pauli principle, and also the general effects associated with the phonon–phonon interaction.

The states corresponding to two-phonon $[2_1^+\otimes 2_1^+]_{0^+,2^+,4^+}$ configurations are well known in many spherical nuclei. It has been shown that the 1^--5^- quintuplet of $[2_1^+\otimes 3_1^-]$ states exists in closed-shell nuclei and nuclei adjacent to them. This, in particular, is true for the 1^- component of this multiplet selectively excited in (γ,γ') experiments (see the preceding paragraph), and fairly complete information about this multiplet has been obtained for ^{144}Nd (Ref. 41). On the other hand, the experimental evidence for the existence of the $[3_1^-\otimes 3_1^-]_{0^+,2^+,4^+,6^+}$ multiplet is rather slight.[42–46] The most suitable candidates are the two nuclei ^{146}Gd and ^{208}Pb. Their lowest excited states have spin and parity 3^-, and so the terms of this multiplet are the states of lowest energy of two-phonon nature in these nuclei.

TABLE V. Properties of the excitation and decay of the 2^+ component of the two-phonon $[3_1^-\otimes 3_1^-]$ multiplet in ^{208}Pb. See the text for details.

	I(Ia, Ib)	II(IIa, IIb)
B(E2,g.s.$\rightarrow[3_1^-\otimes 3_1^-]_{2^+}$), e^2 F^4	10.4 (5.1, 17.7)	40.2 (19.0, 54.6)
Γ_0(E2,$[3_1^-\otimes 3_1^-]_{2^+}\rightarrow$g.s.), meV	6.58 (3.21, 11.2)	25.4 (12.0, 34.5)
$\Gamma_{3_1^-}$(E1,$[3_1^-\otimes 3_1^-]_{2^+}\rightarrow 3_1^-$), meV	14.0 (12.6, 17.0)	13.7 (12.9, 14.3)
$\Gamma_{3_1^-}/\Gamma_0$	2.13 (3.93, 1.52)	0.54 (1.08, 0.41)

In the first stage we assume that the mixing of one- and two-phonon configurations in the low-energy region is negligible. Then the E1 transition between the two-phonon state $|2^+\rangle=[3_1^-\otimes 3_1^-]_{2^+}$ and the one-phonon state 3_1^-, and also the direct decay of the two-phonon state $|2^+\rangle$ to the ground state, are forbidden in models which treat excited states as ideal bosons. Only by using the exact commutation relations between phonons and quasiparticles, i.e., by taking into account the fermionic structure of the phonons, can we obtain nonzero values for these transitions. The reduced probability of E2 decay of the two-phonon state $|2^+\rangle$ to the ground state is described by (20). For the reduced probability of E1 decay $([3_1^-\otimes 3_1^-]_{2^+}\rightarrow 3_1^-)$ we obtain

$$\mathrm{B(E1)}=171.5\left|\sum_{j_1j_2'j''}\langle j_2\|M(E1)\|j_1\rangle u^{(+)}_{j_1j_2}\sum_J(-1)^J\right.$$
$$\times\begin{Bmatrix} j_2 & j_1 & 1\\ j'' & j' & 3\\ 3 & 3 & J\end{Bmatrix} e_{p(n)}\Big[(\psi^{3_1^-}_{j_1j'},\psi^{3_1^-}_{j_2j''}\psi^{3_1^-}_{j''j'},$$
$$+\varphi^{3_1^-}_{j_1j'},\varphi^{3_1^-}_{j_2j''}\varphi^{3_1^-}_{j''j'})\delta_{J,2}+(\psi^{3_1^-}_{j_1j'},\varphi^{3_1^-}_{j_2j''}\varphi^{3_1^-}_{j''j'},$$
$$\left.+\varphi^{3_1^-}_{j_1j'},\psi^{3_1^-}_{j_2j''}\psi^{3_1^-}_{j''j'})(2J+1)\begin{Bmatrix}1 & 3 & 2\\ 3 & 3 & J\end{Bmatrix}\Big]\right|^2, \qquad (21)$$

where $\langle j_2\|M(E1)\|j_1\rangle$ is the reduced matrix element of the electromagnetic transition. The numerical factors in (21) arise as a result of the $(2\lambda+1)$ factors of the phonon operators included in the problem. In the calculations we used the effective charges $e_{p(n)}=1(0)$ and N/A(−Z/A) for E2 and E1 transitions, respectively.

The results of the calculation are shown in column I of Table V. The probability B(E2) of excitation of the $[3_1^-\otimes 3_1^-]_{2^+}$ state from the ground state is about 300 times weaker than the value of B(E2) known from experiment for

the lowest 2^+ state. The calculation reveals a significant partial transition for the decay of this state to the lowest 3^- level. For the latter transition there is also a collective E3 transition with large matrix element $\langle 3_1^-\|\mathrm{E3}\|[3_1^-\otimes 3_1^-]_{2^+}\rangle$ corresponding to phonon annihilation. However, owing to the high multipole order, its contribution to the partial decay width is negligible.

When studying such weak transitions, we should also take into account possible weak admixtures of other configurations which can be excited via the strong, collective transitions allowed in bosonic space. In the region of the two-phonon octupole multiplet in ^{208}Pb, the one-phonon 2_1^+ configuration is obviously such a configuration, since the energy difference between these configurations is only slightly greater than 1 MeV. The mixing of the different configurations in the wave function of the $[3_1^-\otimes 3_1^-]_{2^+}$ state was taken into account by diagonalizing the model Hamiltonian on the basis of the wave functions of the 2^+ states of the form

$$|\Psi_{2^+}\rangle=\left\{\sum_i S_i Q^+_{2^+i}+\sum_{\lambda_1 i_1 \lambda_2 i_2} \times\frac{D^{\lambda_2 i_2}_{\lambda_1 i_1}[Q^+_{\lambda_1 i_1}Q^+_{\lambda_2 i_2}]_{2^+}}{\sqrt{1+\delta_{\lambda_1,\lambda_2}\delta_{i_1,i_2}}}\right\}|\Psi_{\mathrm{g.s.}}\rangle, \tag{22}$$

where i numbers the roots of the RPA equation for each multipole order λ^π. In this calculation we took into account all the one- and two-phonon (constructed from $\lambda^\pi=2^+$, 3^-, and 4^+ phonons) configurations up to excitation energy 13 MeV, i.e., including the isoscalar quadrupole resonance. The diagonalization gives the energy spectrum of the 2^+ states and the coefficients S_i and $D^{\lambda_2 i_2}_{\lambda_1 i_1}$, respectively reflecting the contribution of each one- and two-phonon configuration to the excited-state wave function (22).

The transition probabilities from this calculation are given in column II of Table V. The calculation shows that the contribution of the isoscalar quadrupole resonance is negligible in the low-energy region, but the contribution of a few percent from the one-phonon 2_1^+ configuration to the wave function of the $[3_1^-\otimes 3_1^-]_{2^+}$ state increases its excitation probability by about a factor of four. The width of the decay to the 3_1^- state is practically unchanged, since the amplitude of the matrix element of the E1 transition $\langle 3_1^-\|M(E1)\|2_1^+\rangle$ is of the same order as the matrix element $\langle 3_1^-\|M(E1)\|[3_1^-\otimes 3_1^-]_{2^+}\rangle$.

The reduced probability of the E1 decay $[3_1^-\otimes 3_1^-]_{2^+}\rightarrow 3_1^-$ is 0.73×10^{-3} $e^2\mathrm{F}^2$. This value agrees well with the experimental values $\mathrm{B(E1},[3_1^-\otimes 3_1^-]_{2^+}\rightarrow 3_1^-)=0.95\times 10^{-3}$ $e^2\mathrm{F}^2$ and 1.20×10^{-3} $e^2\mathrm{F}^2$ for the possible candidates ^{96}Zr (Ref. 44) and ^{144}Sm (Ref. 46). It is not surprising that the calculations for ^{208}Pb give a somewhat lower value for the transition than for lighter isotopes. This is related to the fact that the ground-state correlations responsible for the transition matrix element are weaker in the doubly magic lead isotope. This is confirmed by the results of a trial calculation of the strength of this transition for the ^{144}Sm isotope. It agrees well with the experimental data of Ref. 46 and the analogous calculations for this isotope performed using the theory of nuclear fields.[47]

These calculations are extremely sensitive to how collective the 3_1^- state is, which depends on the value of the strength parameter of the residual interaction. To evaluate the reliability of the predictions, we performed additional calculations in which the value of $\mathrm{B(E3,g.s.}\rightarrow 3_1^-)$, which is the input in the calculation to determine the strength of the residual interaction, was artificially varied by $\pm 30\%$ relative to the experimental value. The results of these calculations are given in columns Ia, IIa and Ib, IIb, respectively, of Table V. The γ-decay width of the $[3_1^-\otimes 3_1^-]_{2^+}$ state to the ground state varies by about a factor of two for this variation of the strength parameter, while the width of the decay to the 3_1^- state is stable to within 20%.

The values given in Table V can easily be rescaled to the (γ,γ') cross section. The goal of the proposed experiment is to record transitions to the ground and excited states and determine their spins from the angular correlations $(0^+_{\mathrm{g.s.}}\rightarrow 2^+\rightarrow 0^+_{\mathrm{g.s.}}$ and $0^+_{\mathrm{g.s.}}\rightarrow 2^+\rightarrow 3^-)$ in measurements at two angles (90° and 130°). On the basis of the experience of earlier studies,[48] we can definitely state that the transition from the two-phonon 2^+ state to the ground state can easily be measured using the EUROBALL cluster detector even in the least favorable case (column Ia). Observation of the $2^+\rightarrow 3^-$ transition, which has roughly half the energy of the γ transition, is more problematic owing to the strongly growing contribution of the background in going to lower γ energies in the nuclear resonance fluorescence reaction.

The background expected in the $^{208}\mathrm{Pb}(\gamma,\gamma')$ experiment for maximum energy of the bremsstrahlung spectrum 7 MeV was calculated by the Monte Carlo method using the GEANT program.[49] The two EUROBALL clusters were located at angles of 90° and 130° using a geometry similar to that described in Ref. 48. The photon flux was normalized such that it corresponded to an experiment of a week's duration under the experimental conditions described in Ref. 48. The background spectrum of the ground state, including the efficiency of the cluster detectors and their statistical fluctuations, is shown in Fig. 6 for the photon energy range $E_\gamma=2.52-2.58$ MeV. It can be described by a simple exponential line (the straight line). The effect of the $[3_1^-\otimes 3_1^-]_{2^+}\rightarrow 3_1^-$ transition with photon energy $5.16-2.62=2.54$ MeV is shown by the dotted line as a Gaussian. Its width is taken from the experimentally determined resolution of the cluster module, and its height is normalized to the partial decay width from column II of Table V. We conclude that the transition can be clearly isolated from the reaction background. In spite of the somewhat worse peak-to-background ratio in the measurements at 90°, this is also true there within 3σ error.

5. THE STRUCTURE OF LOW-LYING STATES IN ODD NUCLEI AND ISOMER PHOTOEXCITATION

The problem of isomer photoexcitation[1)] has recently attracted renewed interest.[50–54] The studies in this area have mainly been motivated by the suggestion that the population

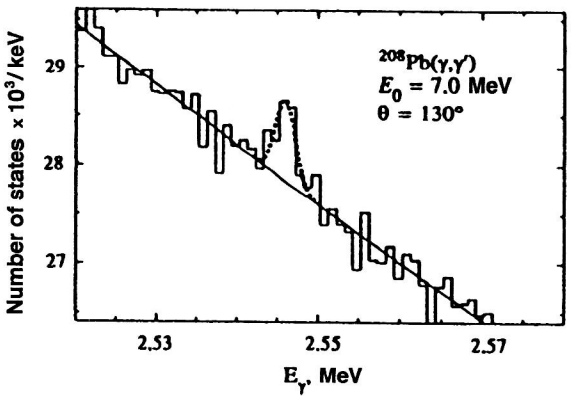

FIG. 6. Monte Carlo calculation of the spectrum of the ^{208}Pb(γ,γ') reaction at 130°. The statistics of the "data" shown as histograms correspond to an experiment of a week's duration under the conditions of Ref. 48. The reaction background is well described by an exponential (sloped line). The peak in the cross section corresponding to the transition $B(E1,[3_1^-\otimes 3_1^-]_{2^+}\rightarrow 3_1^-)$ (dotted line) is represented as a Gaussian with amplitude normalized to the calculated results. See the text for details.

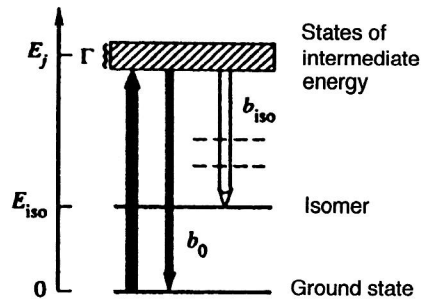

FIG. 7. Schematic representation of the reaction mechanism in which an isomer of energy E_{iso} is populated via states at intermediate energy (shaded region). The intermediate states are characterized by excitation energy E_j and decay width Γ. The partial widths b_0 and b_{iso} describe the decay of the intermediate state to the ground state and to the isomer, respectively. The value of b_{iso} is the sum of all the unknown cascades via which the intermediate state decays to the isomer via the levels shown by the dashed lines.

or decay of isomers be used together with resonance photoabsorption to design a γ laser.[55] Although experiments on isomer photoexcitation have a fifty-year history, surprisingly little is known about the structure of the states at intermediate energies, also called activation states, responsible for isomer population. A detailed discussion of the physics research devoted to the problem of isomer states can be found in Ref. 56.

Most of the work on photoactivation has dealt with either the low-energy region (see, for example, Refs. 57 and 58) $E\leqslant 2$ MeV, or the giant-resonance region,[59–61] in which the statistical properties of γ decay and the competition with other decay channels have been verified. However, experiments at intermediate excitation energies have revealed very interesting regularities. It should be noted that it is this energy range which is most attractive from the viewpoint of designing a γ laser. These regularities are the following for spherical nuclei. It has been shown that the dependence of the isomer yield on the maximum energy of the bremsstrahlung spectrum is linear over an energy range of order 1 MeV. Then there is a sharp jump followed again by linear behavior over a wide energy range. This suggests that there are several activation states connected to the isomer by a fairly simple transition scheme, and reaching these states strongly increases the isomer yield. Despite the relatively high density of excited states at these excitation energies, the number of activation states is quite limited.

The photoexcitation of an isomer via an activation state is shown schematically in Fig. 7. Here we shall discuss the nature of the activation states in the isotopes ^{79}Br (Ref. 62), ^{81}Br (Ref. 63), and ^{89}Y (Ref. 64).

We begin our discussion with the isotope ^{89}Y. It is attractive mainly because there are experimental data for it not only on isomer photoactivation, but also from the nuclear resonance fluorescence reaction. A combined study of these data can allow the reliability of the theoretical predictions to be evaluated. This is because the accuracy with which the energy of excited levels is measured in the nuclear resonance fluorescence reaction is very high, whereas in photoactivation experiments it is of order 200 keV. Moreover, as we shall see below, the cross sections for these two reactions are related to each other. The isotope ^{89}Y is also interesting because it is semimagic. Restricting the configuration space makes it easier to isolate the most important features of the nuclear structure. Also, there is additional information from spectroscopic studies[65] up to relatively high excitation energies. The ground state of ^{89}Y has spin and parity $J^\pi=\frac{1}{2}^-$, and the isomer state with $J^\pi=\frac{9}{2}^+$ has excitation energy $E_{iso}=0.909$ MeV. As for many nuclei in this mass range, the decay of the isomer to the ground state in ^{89}Y is associated with the M4 transition $\frac{1}{2}^-\rightarrow\frac{9}{2}^+$.

The calculated cross section $(\sigma\Gamma)_0^i$ for the photoexcitation of low-lying states in ^{89}Y and the corresponding experimental data from the nuclear resonance fluorescence reaction are given in Fig. 8. The calculations were performed using a wave function containing quasiparticle and quasiparticle⊗phonon components. The phonons of the ^{88}Sr

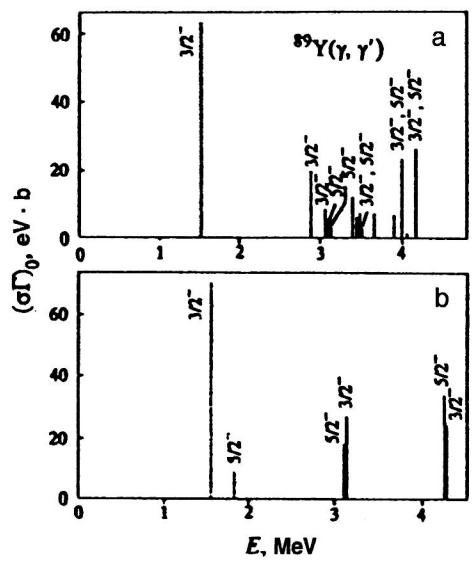

FIG. 8. Comparison of (a) the experimental cross sections $(\sigma\Gamma)_0$ in the reaction ^{89}Y(γ,γ') for decay to the ground state with (b) the calculated results. The spin and parity for the experimental data are taken from Ref. 65.

core were used to calculate the particle levels, and those of ^{90}Zr for the hole levels. In the calculation we included photons of natural parity of multipole order $\lambda^{\pi}=1^{-},\ldots,6^{+}$ up to 12 MeV, but the calculations themselves showed that only collective 2^{+} phonons play an important role in describing photoexcitation up to energies of about 5 MeV, since the interaction of the various configurations is quite weak in this nucleus. The numerical calculations were performed using the PHOQUS program.[66]

Since in photoexcitation a significant contribution to the reaction cross section comes from transitions of low multipole order, we calculated only the spectra of excited states in ^{89}Y connected to the ground state by E1, E2, and M1 transitions. We found only six transitions with energy below 4.5 MeV having a sizeable matrix element. The degree of fragmentation of the states was found to be markedly smaller than observed experimentally, which is due to the restriction of the model space. However, since the contribution of multiphonon configurations to the excitation cross section is negligible, the main features of the results on the (γ,γ') reaction can be explained even at the level of the one-phonon approximation.

The two lowest states in the calculations have energies 1.540 and 1.838 MeV and correspond to the well known lowest levels with $J^{\pi}=\frac{3}{2}^{-}$ and $\frac{5}{2}^{-}$, which, as shown in Ref. 67, are respectively characterized as single-particle $p_{3/2}$ and $f_{5/2}$ levels. The result of the calculation for the $\frac{3}{2}^{-}$ level, $(\sigma\Gamma)_0=70.2$ eV·b, is in excellent agreement with experiment. The E2/M1 mixing coefficient $\delta=-0.254$ is slightly overestimated compared to the experimental value $\delta=-0.139$, which probably indicates overestimation of the admixture of the $[p_{1/2}\otimes 2^{+}_{1}]_{3/2^{-}}$ configuration, which enhances the contribution of the E2 transition. The $\frac{5}{2}^{-}$ state is excited much more weakly and is not seen experimentally. The available data[65] give $(\sigma\Gamma)_0=4.67$ eV·b for it, which also corresponds well with our calculation, being the value of the smaller fluctuation of the reaction background.

The next transitions correspond to a group of practically degenerate states which originate in the pairing of the quasiparticle configuration of the ground state with the low-lying collective quadrupole phonons of the neighboring even–even nucleus ^{90}Zr, i.e., states possessing the structure $[p_{1/2}\otimes 2^{+}_{1,3}]_{3/2^{-},5/2^{-}}$. It should be noted that the energy degeneracy of these states is the result of neglecting more complex configurations in the calculation, and would be lifted if two-phonon configurations were included. The state with energy 3.147 MeV and $J^{\pi}=\frac{3}{2}^{-}$ corresponds to the experimental state at 2.881 MeV and, possibly, the state at 3.067 MeV. At least, the amplitudes of the cross sections suggest this correspondence. The $\frac{5}{2}^{-}$ state in the calculation can reasonably be associated with the group of states fragmented up to 3.5 MeV. The states formed as a result of pairing with the 2^{+}_{3} one-phonon configuration can be identified as the experimental levels at 3.992 and 4.170 MeV.

The structure of these states indicates that the creation of a quadrupole phonon is responsible for the strength of (γ,γ') transitions. Accordingly, the $\frac{1}{2}^{-}\rightarrow\frac{3}{2}^{-}$ transition is primarily an E2 transition. The lowest $\frac{3}{2}^{-}$ state also possesses some M1-excitation strength owing to the 8% admixture of

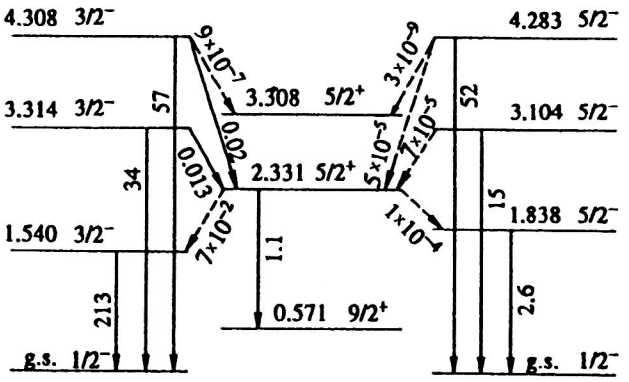

FIG. 9. Calculated level scheme and decay widths for the isotope ^{89}Y. The scheme is limited to only states pertaining to the description of isomer photoexcitation. The $\frac{3}{2}^{-}$ states are on the left, the $\frac{5}{2}^{-}$ states are on the right, and the $\frac{5}{2}^{+}$ states are in the center. The energies of the states are given in MeV and the decay widths in meV. Weak transitions are shown by the dashed lines.

the $p_{1/2}$ single-particle component of the wave function. The dominance of collective E2 transitions explains the good agreement with the data obtained in inelastic nucleon scattering.

In the experiment on isomer photoactivation in ^{89}Y, two jumps were discovered in the dependence of the isomer yield on the maximum energy of the bremsstrahlung spectrum. These jumps at 2.9 and 4.0 MeV indicate that in this nucleus in the energy range from 2.2 to 5.0 MeV there are only two activation states responsible for isomer photoexcitation. Since the energy accuracy is not very good in photoactivation experiments, this can in principle indicate two groups of low-lying states unresolved experimentally. However, the precise data on nuclear resonance fluorescence reject this possibility. Since the spectrum of the (γ,γ') reaction is completely explained by M1 and E2 transitions, the total change of the spin and parity $\Delta J^{\pi}=4^{+}$ in the transition to the final isomer state requires a two-stage cascade including an $E1$ transition to change the parity. In Fig. 9 we show the scheme of selected levels arising in the calculation which satisfy this condition. For the first stage of the cascade decay we restricted ourselves to $\frac{5}{2}^{+}$ states, and two of them were found in the energy range in question. Transitions from $\frac{3}{2}^{-}$ and $\frac{5}{2}^{-}$ states to intermediate states with other values of the spin and parity, which also can in principle be included in the final decay to the isomer, are so weak compared to the transition to the ground state that they were not considered.

Whereas the partial decay widths of the $\frac{3}{2}^{-}$ and $\frac{5}{2}^{-}$ states are essentially comparable, there is a huge difference between the probabilities for their involvement in populating the $\frac{5}{2}^{+}$ state. Decay to the state of higher energy (3.308 MeV) in the model space is extremely weak owing to the practically pure $[p_{1/2}\otimes 3^{-}_{1}]_{5/2^{+}}$ structure of this state. It is allowed only owing to the $2^{+}_{1}\rightarrow 3^{-}_{1}$ transition which, as we know from the preceding discussion, is of next order in smallness compared to the collective transition of one-phonon exchange. States with angular momentum and parity $\frac{3}{2}^{-}$ have small but significant amplitudes for decay to the lowest $5/2^{+}$ states. The widths of the decay of the $\frac{5}{2}^{-}$ states

TABLE VI. Excited states of ^{81}Br from the energy range from 3 to 4.5 MeV with largest values of the cross section for excitation from the ground state $\sigma_{3/2^-\to J_f}$ and contribution of the quasiparticle (α^+) and the principal quasiparticle⊗phonon (α^+Q^+) components to the structure of these states.

J_f	E_x (MeV)	Transition	$\sigma_{3/2^-\to J_f}$ (mb·MeV)	α^+	α^+Q^+
$5/2^+$	3.18	$E1$	0.375	$2d_{5/2}(12.9\%)$	$1g_{9/2}2_1^+(83.0\%)$
$1/2^+$	3.65	$E1$	0.094	$2s_{1/2}(4.34\%)$	$1f_{5/2}3_1^-(94.9\%)$
$3/2^+$	3.75	$E1$	0.002	$1d_{3/2}(2.11\%)$	$2f_{5/2}3_1^-(66.6\%)$
$5/2^+$	3.91	$E1$	0.007	$1d_{5/2}(0.49\%)$	$1f_{5/2}3_1^-(83.9\%)$
$1/2^-$	3.97	$E2$	0.002	$2p_{1/2}(0.01\%)$	$2p_{3/2}2_5^+(99.9\%)$
$3/2^-$	3.97	$E2$	0.005	$2p_{3/2}(0.01\%)$	$2p^{3/2}2_5^+(99.9\%)$
$3/2^-$	4.04	$M1$	0.043	$2p_{3/2}(0.38\%)$	$2p_{3/2}1_1^+(99.0\%)$
$1/2^-$	4.18	$M1$	0.014	$2p_{1/2}(0.78\%)$	$2p_{3/2}1_1^+(99.0\%)$
$3/2^-$	4.27	$M1$	0.002	$2p_{3/2}(0.21\%)$	$2p_{1/2}1_1^+(99.3\%)$
$3/2^+$	4.28	$E1$	0.003	$2d_{3/2}(0.97\%)$	$2p_{3/2}3_1^-(60.8\%)$
$5/2^+$	4.29	$E1$	0.018	$2d_{5/2}(0.46\%)$	$1p_{3/2}3_1^-(51.7\%)$

to the same $\frac{5}{2}^+$ state are considerably weaker compared to those of the $\frac{3}{2}^-$ states, because they have E1-transition matrix elements roughly an order of magnitude smaller. The lowest $\frac{5}{2}^+$ state is strongly coupled to the isomer via the $[g_{9/2}\otimes 2_1^+]$ component of its wave function, and so transitions from $\frac{3}{2}^-$ states are the mechanism responsible for populating the isomer. This result is in complete agreement with the experimental data, which indicate the presence of only two activation states of roughly equal strength, and the calculation reproduces the energy location of these activation states well.

We have also studied the processes responsible for isomer photoexcitation in nuclei with an open shell, ^{79,81}Br. There are no data from the nuclear resonance fluorescence reaction for these isotopes, but, as we shall see below, the theoretical calculations lead to a fairly unambiguous conclusion about the structure of the activation states responsible for the isomer population.

The isomer yield as a function of the maximum energy of the bremsstrahlung spectrum has been measured experimentally in the range from 3 to 4.2 MeV for the isotope ^{81}Br. A single jump at energy 3.45 ± 0.15 MeV was found in the yield curve. The absence of data from the (γ,γ') reaction does not allow us to decide for sure in this case whether we are dealing with a single activation state or a group of closely spaced levels. The latter is possible in principle, especially in view of the fact that we can expect stronger fragmentation of configurations in the transitional nucleus Br than in the isotope ^{89}Y.

To determine the structure of the activation state of ^{81}Br, we calculated the spectrum of excited states in the energy range from 3 to 4.5 MeV using a wave function containing quasiparticle and quasiparticle⊗phonon components. The ground state of ^{81}Br is a level with quantum numbers $\frac{3}{2}^-$. We therefore calculated the spectrum of states with $J^\pi=\frac{1}{2}^\pm$, $\frac{3}{2}^\pm$, and $\frac{5}{2}^\pm$, which can be excited from the nuclear ground state via the E1, M1, or E2 components of the electromagnetic field. In addition to the excitation energy and structure of the excited states, we also calculated the cross sections for their photoexcitation from the ground state. The states whose cross sections $\sigma_{3/2^-\to J_f}$ are not vanishingly small are given in Table VI. In this table we also give the contributions of the quasiparticle (α^+) and principal quasiparticle⊗phonon (α^+Q^+) components to the structure of these states.

Our calculations show that the energy range from 3.0 to 4.5 MeV in ^{81}Br contains excited states characterized by small admixture of the one-quasiparticle component in the normalization of the wave function. Therefore, valence transitions to these states from the ground state are strongly suppressed. Transitions with collective-phonon exchange, which have large values of B(E(M)λ), are also suppressed. The suppression is purely energetic. The collective 2_1^+ phonon has too low an energy for the energy range in question, whereas the 1^+ phonon forming the M1 resonance is too high, as are even the noncollective 1^- phonons. The exceptions are the state with angular momentum and parity $J^\pi=\frac{5}{2}^+$ and excitation energy $E_x=3.18$ MeV and, to some extent, the state with $J^\pi=\frac{1}{2}^+$ and $E_x=3.65$ MeV, which contain a significant contribution of the quasiparticle component in the normalization of their wave functions.

Let us discuss the state with $J^\pi=\frac{5}{2}^+$ and $E_x=3.18$ MeV in more detail. The reduced probability for its excitation from the ground state is 0.03 e^2F^2 and is determined exclusively by the valence E1 transition $\frac{3}{2}^-\to\frac{5}{2}^+$. The surprising feature of this state is the presence of a sizeable admixture of the single-particle component in its wave function. The one-quasiparticle level $\pi(2d_{5/2})$ lies considerably higher; in our calculations it has energy 7.1 MeV, but owing to the interaction of the quasiparticle and quasiparticle⊗phonon configurations, a significant part of the strength of this level is pushed to lower energies. This effect is clearly seen in Fig. 10, where we show the fragmentation of the $\pi(2d_{5/2})$ one-quasiparticle component among states with angular momentum and parity $J^\pi=\frac{5}{2}^+$. The low-energy peak in this distribution forms the activation state observed experimentally. An additional argument (along with the large value of the excitation cross section $\sigma_{J_i\to J_f}$) in favor of this statement is the principal quasiparticle⊗phonon component, which contributes more than 80% to the wave function of this state. The quasiparticle part of this component has quantum numbers $\frac{9}{2}^+$, and so this component is coupled via collective E2 decay to the $\frac{9}{2}^+$ isomer whose yield was measured experimentally.

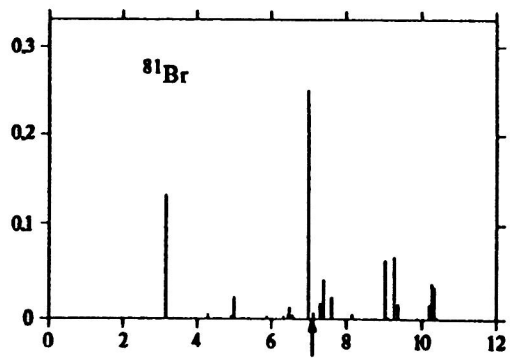

FIG. 10. Distribution of the strength of the quasiparticle component $\pi(2d_{5/2})$ among excited states with $J^\pi=\frac{5}{2}^+$ in ^{81}Br. The line with the arrow indicates the position of the one-quasiparticle level $\pi(2d_{5/2})$.

Let us now consider the decay of the state with $J^\pi=\frac{5}{2}^+$ and $E_x=3.18$ MeV to the $\frac{9}{2}^+$ isomer state. In our calculations the lowest $\frac{9}{2}^+$ state has excitation energy 1.63 MeV and consists of the one-quasiparticle configuration $1g_{9/2}$ (64%) and the configuration $[1g_{9/2}\otimes 2_1^+]_{9/2^+}$ (30%). The experimental value of the isomer energy in ^{81}Br is 536 keV. Below we shall discuss in detail the effect of including configurations of the type quasiparticle⊗2 phonons on the properties of low-lying states in odd nuclei. It will be shown that the inclusion of these configurations significantly improves the description of the energy location of low-lying levels. In particular, their inclusion in ^{81}Br lowers the energy of the lowest $\frac{9}{2}^+$ state to 0.87 MeV, significantly closer to the experimental value, while the location of the $\frac{5}{2}^+$ activation state is essentially unchanged. The direct transition between these $\frac{5}{2}^+$ and $\frac{9}{2}^+$ states is largely (~90%) due to the exchange of a collective 2_1^+ phonon and is $B(E2\downarrow)=386\ e^2F^4$. We can use this value to estimate the isomer ratio assuming that the main contribution to Γ_{iso} comes from the direct collective transition to the isomer state, while that to Γ comes from the transition to the ground state, i.e., $\Gamma=\Gamma_0$. We then obtain $\Gamma_{iso}/\Gamma=6\times10^{-2}$. The estimated total cross section for the production of the nucleus in the isomer state via the $\frac{5}{2}^+$ level with $E_x=3.18$ MeV for this value of Γ_{iso}/Γ is of order 20 μb·MeV, which agrees well with the experimental value of 5 μb·MeV in view of the fact that the experimental value has an error of about a factor of 3, mainly owing to the uncertainty in the intensity of the photon beam.

Regarding the state with $J^\pi=\frac{1}{2}^+$ and $E_x=3.65$ MeV, whose excitation probability is four times smaller than that for the state with $E_x=3.18$ MeV, its contribution to the total cross section for isomer photoexcitation is negligible owing to the large difference in spin from the isomer ($\Delta J=4$) and the structure of its wave function.

The picture of the photoexcitation of the $\frac{9}{2}^+$ isomer for the isotope ^{79}Br is very reminiscent of that for the neighboring isotope ^{81}Br. The calculation predicts the presence of two activation states in the energy range from 0 to 4 MeV. The first state with $J^\pi=\frac{7}{2}^-$ located at excitation energy 1.1 MeV has wave function

$$\Psi\left(\frac{7^-}{2}\right)=(0.34)2f_{7/2}+(0.85)[2p_{3/2}\otimes 2_1^+]_{7/2^-}+\cdots . \quad (23)$$

This state is excited owing to the collective 2_1^+ phonon connecting the state (23) to the $\frac{3}{2}^-$ ground state of the nucleus. It decays to the isomer via the valence $E1$ transition $2f_{7/2}\rightarrow 1g_{9/2}$. A $\frac{7}{2}^-$ level of energy 0.761 MeV and also a level at 1.8 MeV, which is assumed to have the same spin and parity, are known experimentally. Assuming that the state (23) (which naturally will fragment when the coupling to more complex configurations is taken into account) corresponds to these two experimental levels, we obtain very good agreement between the absolute value of the isomer photoexcitation cross section near the maximum bremsstrahlung energy up to 2 MeV and the experimental data.

The strong activation state near 3.2 MeV with $J^\pi=\frac{5}{2}^+$ is the analog of the corresponding state in ^{81}Br, discussed in detail earlier. In ^{79}Br its wave function has the form

$$\Psi\left(\frac{5^+}{2}\right)=(0.38)2d_{5/2}+(0.90)[1g_{9/2}\otimes 2_1^+]_{5/2^+}+\cdots , \quad (24)$$

and its excitation and decay to the isomer are the opposite compared to the state (23): the valence E1 transition $2p_{3/2}\rightarrow 2d_{5/2}$ for excitation to the isomer and collective E2 decay to the isomer.

CONCLUSION

We have reviewed the theoretical studies on the structure of low-lying states in spherical nuclei based on use of the quasiparticle–phonon model of the nucleus, and have compared the calculated results with the latest available experimental data obtained for various nuclear reactions. We have studied the interaction of simple (one-phonon) and complex (multiphonon) components of the excited-state wave functions in detail and the changing role of this interaction in determining the properties of these states in going from closed-shell nuclei to transitional nuclei. We have shown that this model gives a good quantitative description of the large amount of recent experimental data on the properties of these states obtained in various nuclear reactions.

This study was supported by the Russian Fund For Fundamental Research, grant No. 96-15-96729.

[1)] An isomer is an excited state located near the ground state of a nucleus, but with greatly different angular momentum. As a result, isomer decay to the ground state is strongly suppressed by the high multipole order of the electromagnetic transition, which means that the isomer has a relatively long lifetime.

[1] V. G. Solov'ev, *Theory of the Nucleus. Quasiparticles and Phonons* (Institute of Physics, Bristol, 1992) [Russ. original, Énergoatomizdat, Moscow, 1989].
[2] A. I. Vdovin and V. G. Solov'ev, Fiz. Élem. Chastits At. Yadra **14**, 237 (1983) [Sov. J. Part. Nucl. **14**, 99 (1983)].
[3] V. V. Voronov and V. G. Solov'ev, Fiz. Élem. Chastits At. Yadra **14**, 1380 (1983) [Sov. J. Part. Nucl. **14**, 583 (1983)].
[4] V. Yu. Ponomarev *et al.*, Nucl. Phys. A **323**, 446 (1979).
[5] R. K. J. Sandor, PhD Thesis, Free Univ. of Amsterdam (1991).
[6] R. K. J. Sandor *et al.*, Phys. Lett. B **233**, 54 (1989).
[7] R. K. J. Sandor *et al.*, Nucl. Phys. A **535**, 669 (1991).
[8] R. Perrino *et al.*, Nucl. Phys. A **561**, 343 (1993).

[9] R. K. J. Sandor *et al.*, Nucl. Phys. A **551**, 378 (1993).
[10] J. B. J. M. Lanen, PhD Thesis, Univ. of Utrecht (1990).
[11] A. I. Vdovin and Ch. Stoyanov, Izv. Akad. Nauk SSSR, Ser. Fiz. **38**, 119 (1974) [Bull. Acad. Sci. USSR, Phys. Ser.].
[12] W. P. Jones *et al.*, Phys. Rev. C **4**, 580 (1971).
[13] D. Karadjov, V. V. Voronov, and F. Catara, Phys. Lett. B **306**, 197 (1993); J. Phys. G **20**, 1431 (1994).
[14] L. Trache *et al.*, Nucl. Phys. A **492**, 23 (1989).
[15] M. Pignanelli *et al.*, Nucl. Phys. A **559**, 1 (1993).
[16] U. Götz *et al.*, Nucl. Phys. A **192**, 1 (1972).
[17] J. E. Wise *et al.*, Phys. Rev. C **45**, 2701 (1992).
[18] W. Kim *et al.*, Phys. Rev. C **45**, 2290 (1992).
[19] W. Kim *et al.*, Phys. Rev. C **44**, 2400 (1991).
[20] V. Yu. Ponomarev *et al.*, Nucl. Phys. A **549**, 180 (1992).
[21] M. Grinberg and Ch. Stoyanov, Nucl. Phys. A **573**, 231 (1994).
[22] M. Pignanelli *et al.*, Nucl. Phys. A **519**, 567 (1990).
[23] M. Pignanelli *et al.*, Nucl. Phys. A **540**, 27 (1992).
[24] Y. Fujita *et al.*, Phys. Rev. C **40**, 1595 (1989).
[25] A. Arima and F. Iachello, Ann. Phys. (N.Y.) **111**, 201 (1978).
[26] N. I. Pyatov, M. I. Baznat, and D. I. Salamov, Yad. Fiz. **25**, 1155 (1977) [Sov. J. Nucl. Phys. **25**, 613 (1977)]; N. I. Pyatov and M. I. Baznat, Yad. Fiz. **30**, 1219 (1979) [Sov. J. Nucl. Phys. **30**, 634 (1979)].
[27] V. V. Voronov, D. T. Khoa, and V. Yu. Ponomarev, Izv. Akad. Nauk SSSR, Ser. Fiz. **48**, 1846 (1984) [Bull. Acad. Sci. USSR, Phys. Ser.].
[28] R. F. Metzger, Phys. Rev. C **14**, 543 (1976).
[29] C. P. Swann, Phys. Rev. C **15**, 1967 (1977).
[30] R. F. Metzger, Phys. Rev. C **18**, 2138 (1978).
[31] P. Vogel and L. Kocbach, Nucl. Phys. A **210**, 221 (1971).
[32] H. H. Pitz *et al.*, Nucl. Phys. A **509**, 587 (1990).
[33] R.-D. Herzberg *et al.*, Phys. Lett. B **390**, 49 (1997).
[34] R. M. Laszewski *et al.*, Phys. Rev. C **34**, R2013 (1986).
[35] V. G. Soloviev, Ch. Stoyanov, and V. V. Voronov, Nucl. Phys. A **304**, 503 (1978).
[36] A. Wolf *et al.*, Phys. Rev. C **6**, 2276 (1972).
[37] J. Tenenbaum, R. Moreh, and A. Nof, Nucl. Phys. A **218**, 95 (1974).
[38] A. Bohr and B. R. Mottelson, *Nuclear Structure*, Vol. 2 (Benjamin, New York, 1975) [Russ. transl., Mir, Moscow, 1977].
[39] T. Marumori *et al.*, Prog. Theor. Phys. **31**, 1009 (1964).
[40] J. Enders *et al.*, Nucl. Phys. A **612**, 239 (1997).
[41] S. J. Robinson *et al.*, Phys. Rev. Lett. **73**, 412 (1994).
[42] P. Kleinheinz *et al.*, Phys. Rev. Lett. **48**, 1457 (1982).
[43] S. Lunardi *et al.*, Phys. Rev. Lett. **53**, 1531 (1984).
[44] G. Molnár *et al.*, Nucl. Phys. A **500**, 43 (1989).
[45] D. F. Kusnezov, E. A. Henry, and R. A. Meyer, Phys. Lett. B **228**, 11 (1989).
[46] R. A. Gatenby *et al.*, Phys. Rev. C **41**, R414 (1990).
[47] E. Müller-Zanotti *et al.*, Phys. Rev. C **47**, 2524 (1993).
[48] P. von Brentano *et al.*, Phys. Rev. Lett. **76**, 2029 (1996).
[49] R. Brun *et al.*, The GEANT3 Program, Report DD/EE/84-1, CERN, Geneva (1995).
[50] J. A. Abderson *et al.*, Phys. Rev. C **38**, 2838 (1988).
[51] C. B. Collins *et al.*, Phys. Rev. C **42**, R1813 (1990).
[52] J. J. Carroll *et al.*, Phys. Rev. C **43**, 897 (1991).
[53] J. J. Carroll *et al.*, Phys. Rev. C **43**, 1238 (1991).
[54] P. von Neumann-Cosel *et al.*, Phys. Lett. B **266**, 9 (1991).
[55] C. B. Collins *et al.*, J. Appl. Phys. **53**, 4645 (1982).
[56] Yu. P. Gangrskiĭ, A. P. Tonchev, and N. P. Balabanov, Fiz. Élem. Chastits At. Yadra **27**, 1043 (1996) [Phys. Part. Nuclei **27**, 428 (1996)].
[57] E. C. Booth and J. Brownson, Nucl. Phys. A **98**, 529 (1967).
[58] Á. Veres, At. Energ. Rev. **18**, 281 (1980).
[59] Z. M. Bigan *et al.*, Yad. Fiz. **49**, 913 (1989) [Sov. J. Nucl. Phys. **49**, 567 (1989)].
[60] L. Z. Dzhilavyan *et al.*, Yad. Fiz. **51**, 336 (1990) [Sov. J. Nucl. Phys. **51**, 215 (1990)].
[61] J. Sáfár *et al.*, Phys. Rev. C **44**, 1086 (1991).
[62] J. J. Carroll *et al.*, Phys. Rev. C **48**, 2238 (1993).
[63] V. Yu. Ponomarev *et al.*, J. Phys. G **16**, 1727 (1990).
[64] M. Huber *et al.*, Nucl. Phys. A **559**, 253 (1993).
[65] H. Sieversf, Nucl. Data Sheets **58**, 351 (1989).
[66] Ch. Stoyanov and Ch. Z. Kkhong, Preprint R-4-81-234, JINR, Dubna (1981) [in Russian].
[67] A. Stuirbank *et al.*, Z. Phys. A **297**, 307 (1980).
[68] P. von Neumann-Cosel *et al.*, Z. Phys. V. A **350**, 303 (1995).

Translated by Patricia A. Millard